



Review

# A Review of Biomass Wood Ash in Alkali-Activated Materials: Treatment, Application, and Outlook

Yiying Du <sup>1</sup>, Ina Pundienė <sup>1,\*</sup>, Jolanta Pranckevičienė <sup>1</sup>, Modestas Kligys <sup>1</sup>, Giedrius Girskas <sup>1</sup>  
and Aleksandrs Korjakins <sup>2</sup>

- <sup>1</sup> Laboratory of Concrete Technology, Institute of Building Materials, Vilnius Gediminas Technical University, Linkmenu St. 28, LT-08217 Vilnius, Lithuania; yiying.du@vilniustech.lt (Y.D.); jolanta.pranckeviciene@vilniustech.lt (J.P.); modestas.kligys@vilniustech.lt (M.K.); giedrius.girskas@vilniustech.lt (G.G.)
- <sup>2</sup> Institute of Materials and Structures, Faculty of Civil and Mechanical Engineering, Riga Technical University, Kipsalas St. 6A, LV-1048 Riga, Latvia; aleksandrs.korjakins@rtu.lv
- \* Correspondence: ina.pundiene@vilniustech.lt; Tel.: +370-67514976

**Abstract:** The utilisation of Portland cement has aroused tremendous concerns owing to its production exerting a lot of pressure on the environment. Alternative eco-binders have been developed to replace it, among which alkali-activated materials (AAMs) have drawn great attention, especially due to the possibility of encompassing industrial and agricultural waste, which significantly improves the sustainability and cost-efficiency of the material. Biomass wood ash (BWA) is a by-product generated from power plants and, along with the advocacy for biomass fuel as a renewable energy resource, there have been increasing applications of BWA in building and construction materials. This review examines the use of BWA as a precursor source in AAMs. Due to its low chemical and hydraulic reactivity, more active binary precursors are usually introduced to guarantee mechanical properties. Whereas the increment of BWA content can have a negative influence on material strength development, it is still a promising and feasible material, and new approaches should be developed to improve the effectiveness of its utilisation. Currently, study of BWA-based AAMs is still in the beginning stages and more research is needed to investigate the effects of BWA characteristics on the property evolution of AAMs, focusing on the durability and analysis of eco-efficiency. Overall, this review provides a comprehensive overview of the characterisation of BWA and its potential applications in AAMs, and meanwhile, based on the analysis of present research trends, proposes some prospective directions for future research.

**Keywords:** alkaline activation; biomass; characterisation; workability; density; mechanical properties; microstructure; porosity; water absorption; eco-efficiency



**Citation:** Du, Y.; Pundienė, I.; Pranckevičienė, J.; Kligys, M.; Girskas, G.; Korjakins, A. A Review of Biomass Wood Ash in Alkali-Activated Materials: Treatment, Application, and Outlook. *J. Compos. Sci.* **2024**, *8*, 161. <https://doi.org/10.3390/jcs8050161>

Academic Editor: Francesco Tornabene

Received: 16 March 2024  
Revised: 15 April 2024  
Accepted: 23 April 2024  
Published: 25 April 2024



**Copyright:** © 2024 by the authors. Licensee MDPI, Basel, Switzerland. This article is an open access article distributed under the terms and conditions of the Creative Commons Attribution (CC BY) license (<https://creativecommons.org/licenses/by/4.0/>).

## 1. Introduction

Owing to its excellent mechanical strength, good durability, and low costs, Portland cement (PC) has been used worldwide as the most common binder material for building and construction to fabricate concrete or precast elements. However, despite its outstanding engineering properties and mass application, the environmental threats posed by its production have aroused tremendous concerns, particularly intensive energy consumption and high greenhouse gas emissions. According to Huntzinger and Eatmon [1], as well as Frías et al. [2], the manufacturing of PC corresponds to approximately 5 to 7% of the global emissions of anthropogenic carbon dioxide (CO<sub>2</sub>) and 10% of industrial energy demand. To deal with the climate crisis, it is essential to decrease anthropogenic CO<sub>2</sub> emissions produced by human activities such as fossil fuel burning and PC production [3]. Thus, following sustainable development around the globe, it is important to replace PC with alternative green binder materials. In this context, alkali-activated materials (AAMs) have gained an umbrella concentration in the investigations into building materials and are

regarded as potential substitutes for PC due to their low environmental impact, low energy requirements, and good mechanical performance [4,5]. Compared to PC fabrication, the manufacturing of AAMs can reduce CO<sub>2</sub> emissions by up to 80% [6,7], which significantly improves the sustainability of the material.

AAMs are a category of inorganic material produced via the activation of aluminosilicate precursors with alkali media such as hydroxide, silicates, and carbonates [8,9]. Based on the source of the precursors and the type of alkali activators, they can be alternatively referred to as “geopolymers” or “inorganic polymers” [10]. There are three categories of alkali-activated composites, including high-calcium composites, low-calcium composites, and hybrid cements composed of both high and low calcium. The types of alkali solutions play an elemental role in the properties and characteristics of AAMs. They are usually aqueous solutions comprised of alkaline elements such as sodium (Na), potassium (K), and calcium (Ca), together with hydroxides, carbonates, silicates, or sulphates [11,12]. In the current research, Na- and K-based activators are most welcomed due to the advantages of their cost and availability of acquisition, particularly sodium silicate (NaSiO<sub>3</sub>), sodium hydroxide (NaOH), and potassium hydroxide (KOH). Some researchers have also used calcium hydroxide (Ca(OH)<sub>2</sub>), which is more environmentally friendly, for activating the precursors and pointed out its effectiveness in promoting the formation of calcium aluminium silicate hydrate (CASH) and forming a dense binder microstructure [13,14].

Precursors are usually the solid components in AAMs and mainly consist of silicon dioxide (SiO<sub>2</sub>), aluminium oxide (Al<sub>2</sub>O<sub>3</sub>), and calcium oxide (CaO) [15]. The source materials of precursors can come from natural aluminosilicate materials and also can include a wide range of industrial and agricultural by-products like coal fly ash (FA), ground granulated blast-furnace slags (GGBFS), rice husk ash, etc. In contrast to PC, which consumes a large quantity of non-renewable natural resources, this kind of utilisation of waste greatly benefits the conservation of the environment, energy, and natural resources and can further reduce the production costs of the materials [15,16]. In contrast with other types of industrial waste, such as fly ash and slags, that have been extensively studied as the primary source for producing AAMs [17–24], investigations into the application of biomass ash (BA) are comparatively limited. However, along with the global focus on renewable energy, the utilisation of BA has great potential for future research. BA is the residual matter from the combustion of forestry or agricultural leftovers (wood, crops, and agricultural remnants) burnt at various temperatures and time durations [25,26]. According to Silvestro et al. [27], biomass is the energy source for 10.3% of the global annual primary energy supply. As a sustainable and reliable energy source, it has been developing rapidly and is projected to take up the bulk of global energy supplies [28]. Nevertheless, the generation of every 493 TWh of energy corresponds to an estimated amount of 10 million tons of ash [29]. In practice, most of this ash is disposed of in landfills, with only a tiny amount reused, which imposes significant burdens on land resources and the environment. In this context, the application of BA in fabricating building and construction materials can convert waste into valuable raw materials and is a sustainable move to ameliorate the environmental threats resulting from the disposal of this waste, which has given rise to critical problems for government agencies.

To date, the reuse of BA waste has gradually attracted growing attention in engineering fields, and some available investigations are testifying to its feasibility and profitability as a precursor to producing AAMs [30–38]. In recent years, a few reviews have been published focusing on a variety of types of BA such as rice husk ash, sugar cane bagasse ash, and palm oil ash [4,9,10,30,39–41]. These reviews analysed the current application states as well as the challenges to incorporating BA in AAMs from comprehensive perspectives, covering the fabrication method, characterisation technologies, and physicochemical mechanisms, offering an integrated overview of current research and knowledge and, meanwhile, critically indicating the existing gaps. Nonetheless, most of these existing reviews mainly involve alkali-activated agricultural ashes, and analysis of biomass wood ash (BWA) is rarely considered, even though it is abundantly generated in northern European countries

where wood is the main source of biomass fuel energy. Although the state-of-the-art BWA applied in AAMs is mentioned in several reviews regarding the utilisation of BWA in civil engineering domains [42–45], most of them mainly focus on the effects of BWA as a supplementary cementitious material in cement-based materials (CBMs) [42–50], and a comprehensive review of BWA-based AAMs is still lacking. On the one hand, according to the conducted research on the effects of BWA replacement in CBMs, the incorporation of BWA deteriorates the engineering properties of the material. It leads to an increase in the amount of water required to produce pastes with the desired consistency and significantly delays the cement's setting time, and this effect is more significant as the amount of ash substituted for PC increases [51–53]. Meanwhile, along with the increasing content of BWA in the binder, a decrease in compressive and flexural strength is observed [54–56]. BWA is characterised by uneven particle size composition and low pozzolanic activity, and negatively affects the strength properties of PC. It is concluded that partial substitution of PC with BWA can be done only at a level of up to 20% to maintain an acceptable mechanical strength. On the other hand, considering the world's increasing proportion of bio-energy usage, it is essential to find more sustainable ways to cope with BWA instead of landfills and reuse in the civil engineering field, and practically turn waste into valuable materials. Thus, it is promising and practical to explore the utilisation of BWA in AAMs for providing a new perspective on more effective application of BWA. In this review, the recent development of alkali-activated BWA materials is outlined and analysed to provide an extensive view of the sustainable reuse of BWA waste. The conventional properties and the mechanisms determining the performance evolution are addressed, with particular attention paid to pointing out the existing research limits and future investigation frameworks to promote the reuse and application of BWA as a renewable building and construction material.

## 2. Characterisation of Biomass Wood Ash

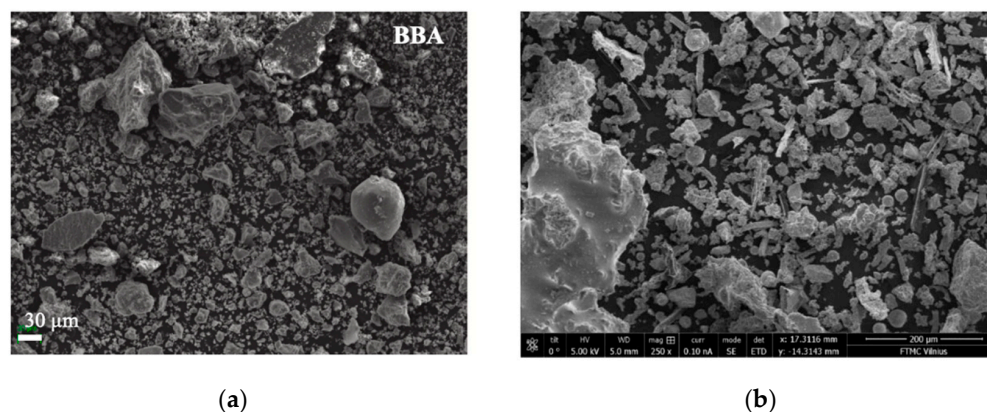
The composition of BWA varies according to its sources and heavily depends on the biomass of the plants. This ash commonly contains many crystalline phases, accompanied by inorganic amorphous phases and organic matter [57]. Based on the procedure of biomass combustion, there are elementally two categories of solid waste ash: biomass bottom ash (BBA), which is the combination of fully and partially burnt materials discharged during combustion, as well as biomass fly ash (BFA), collected from the system of controlling air pollution [58]. Figure 1 shows the macromorphology of various BWAs gathered from biomass combustion in five power plants [59]. It can be seen from the photograph that the macroscopic features of the ashes differ due to the combustion settings and plant conditions. However, they all include unburnt wood residues, which can be clearly observed. The colour of the BBA is darker than the BFA from the same plant and has a smaller quantity of fine-grained and homogeneous particles. Heterogeneous debris with large diameters can be clearly seen, especially for the wood-chip BBA of Colmar and Rixheim. Usually, compared to BBA, BFA consists of smaller particles and more glassy phases, and is of higher reactivity in the application [60]. Thus, more literature reports utilising BFA as a precursor material for producing AAMs and geopolymers [61,62]. However, some authors also pointed out that decreasing the particle size of BBA was feasible to increase its surface area and reactivity [58,63]. The typical micromorphology of BWA is presented in Figure 2. It can be seen in both graphs that the BWA particles have heterogeneous shapes mixed together with some spherical particles under the microscope, and the unburnt wood parts are noticeable.

Table 1 concludes the raw material properties of the wood ashes used to produce AAMs in the five years of the literature (2019–2023) reviewed in this study, as well as their biomass sources. The physical and chemical properties of BWA vary according to the difference in wood source, combustion location, and burning process. The density of the wood ash lies in the range from 0.68 to 3.05 g/cm<sup>3</sup>, and BFA is measured as having a lower density than BBA. The mean value of the density is 2.29 g/cm<sup>3</sup>, and the maximum is reported by [64], with a value of 3.05 g/cm<sup>3</sup>. A great distinguishment in the specific surface

area is observed, with a mean value of  $1.92 \text{ m}^2/\text{g}$ . The maximal and the minimal specific surface areas in the analysed investigations are  $13.94$  and  $0.10 \text{ m}^2/\text{g}$ , respectively [27,65]. Usually, the specific area of a material is a significant index for defining its reactivity during the pozzolanic and hydration processes. The use of BWA with a higher specific area contributes to higher yield stress, viscosity, and reactivity of BWA geopolymers [27]. These data indicate that the reported ashes have differing potential to be incorporated into AAMs, tremendously affecting the mechanical behaviours of BWA-based AAMs. The loss of ignition (LOI) varies from 2.66 to 74.31% for different ashes, and the mean value is 21.01%. LOI shows the content of organic residues in the ashes. A high value of LOI can be attributed to incomplete wood combustion and the decomposition of hydrated as well as carbonated wood ash phases [66,67]. When the value is greater than 12%, the pozzolanic activity of the material reduces owing to the high amount of unburnt carbon, which also adversely impacts mechanical properties and durability and delays the hydration process of ash-based composites [53,68,69].



**Figure 1.** Macro-features of BFA (top row) and BBA (bottom row) from different biomass plants [59].



**Figure 2.** Macro-graphs of (a) BBA [58] and (b) BFA [61].

In terms of the mineralogical compounds, except for the eucalyptus BWA used by Silva et al. [65], quartz ( $\text{SiO}_2$ , silica oxide) and calcite ( $\text{CaCO}_3$ , calcite) are highlighted as the main components in most of the researches. The other primary identified mineral phases consist of portlandite ( $\text{Ca(OH)}_2$ , calcium hydroxide), lime ( $\text{CaO}$ , calcium oxide), and Al- or Si-based compounds. Figure 3 shows the X-ray diffraction (XRD) patterns of a typical BWA. Besides the crystalline phases, an amorphous halo is identified around  $22.0^\circ \text{C}$ , which is associated with the organic matter in the ashes [84].

**Table 1.** Summary of the material characteristics of the BWA used in AAMs.

Ash Category	Biomass Source	Specific Surface Area/(m <sup>2</sup> /g)	Density/(g/cm <sup>3</sup> )	Chemical Composition/wt%									CaO/SiO <sub>2</sub> Ratio	Basic Oxide/Acidic Oxide Ratio	Mineralogical Composition	Reference
				LOI	SiO <sub>2</sub>	Al <sub>2</sub> O <sub>3</sub>	CaO	MgO	Fe <sub>2</sub> O <sub>3</sub>	Na <sub>2</sub> O	K <sub>2</sub> O	P <sub>2</sub> O <sub>5</sub>				
BBA	Forest biomass Jaen, Spain	-	-	5.58	46.10	12.04	19.65	3.71	4.78	0.78	4.59	1.12	0.43	0.77	Quartz, calcite, lime, aluminosilicates	[58]
BBA	Cedar chips Taiwan, China	0.67	-	-	18.33	3.88	26.29	5.04	2.48	-	11.42	-	1.43	1.92	Quartz, calcite, portlandite	[70]
BWA	Pine sawdust and chips	0.30	1.86	74.31	9.51	2.67	5.87	1.69	2.65	-	1.42	0.89	0.62	1.08	Quartz, calcite	[27]
BWA	Cacador, Brazil Pine sawdust and chips	0.10	2.34	31.50	25.06	12.28	9.90	2.60	8.05	1.33	3.99	1.60	0.40	0.99	Quartz, calcite	[27]
BWA	Cacador, Brazil Pine sawdust and chips	0.21	2.09	58.59	21.56	10.73	4.60	1.36	7.82	0.12	3.03	0.85	0.21	0.77	Quartz, calcite	[27]
Treated BFA	Wood pellet plant	0.44	2.7	-	3.97	1.18	53.33	8.67	1.44	0.09	4.19	5.01	13.16	15.91	-	[71]
Non-treated BFA	Wood pellet plant	0.37	2.6	-	3.22	1.07	42.38	4.87	1.31	0.11	4.57	3.23	13.43	15.01	-	[71]
BBA	Radviliskis, Lithuania	0.40	-	4.06	22.40	2.51	49.00	8.29	2.18	0.28	8.69	5.05	2.19	2.67	Quartz, portlandite, anorthoclase, gehlenite	[72–74]
BWA	Eucalyptus chips Nestle SA, Brazil	13.84	1.98	29.72	1.76	5.06	43.80	8.36	2.43	0.28	4.64	3.32	24.89	32.51	Calcite, lime, portlandite, periclase, sylvite	[65]
BFA	Krosno, Poland	1.88	2.58	5.88	12.70	3.50	46.05	3.70	3.40	-	9.00	4.0	3.66	4.19	Portlandite, quartz, calcite, syngenite, sylvite, kalsilite, hydroxylapatite	[75]
BFA	Pine chips Vilnius, Lithuania	0.49	0.68	-	22.91	2.63	31.50	3.57	2.32	0.26	4.00	2.71	1.37	1.65	Quartz, portlandite, lime, calcite	[61]
BFA	Portugal	-	3.05	6.39	38.5	14.8	16.7	3.44	5.94	1.53	5.97	1.12	0.43	0.91	Mica, quartz, calcite,	[64]
BWA	-	-	-	-	19.00	2.51	60.50	1.97	3.28	-	4.44	-	3.18	3.42	microcline Quartz, calcite	[76]

Table 1. Cont.

Ash Category	Biomass Source	Specific Surface Area/(m <sup>2</sup> /g)	Density/(g/cm <sup>3</sup> )	Chemical Composition/wt%									CaO/SiO <sub>2</sub> Ratio	Basic Oxide/Acidic Oxide Ratio	Mineralogical Composition	Reference
				LOI	SiO <sub>2</sub>	Al <sub>2</sub> O <sub>3</sub>	CaO	MgO	Fe <sub>2</sub> O <sub>3</sub>	Na <sub>2</sub> O	K <sub>2</sub> O	P <sub>2</sub> O <sub>5</sub>				
BWA	Timber wood Perak, Malaysia	6.26	2.40	18.00	2.70	1.30	61.00	8.70	1.30	-	12.00	2.70	22.59	26.30	Quartz, calcite, portlandite, mullite, potassium aluminate	[77]
BWA	Michoacan state, Mexico	-	-	-	0.98	1.51	44.81	3.81	1.19	1.64	6.89	1.72	45.72	33.20	Quartz, calcite	[78]
BFA	Portugal	-	-	2.66	34.00	13.5	16.5	3.1	5.0	1.5	5.5	-	0.49	2.45	Quartz, calcite	[79]
BBA	Olive tree and forest, Jaén, Spain	-	2.546	5.58	46.10	12.04	19.65	3.71	4.78	0.78	4.59	1.12	0.43	0.77	Lime, quartz, calcite, aluminosilicates	[80]
BFA	Pitea, Sweden	-	-	29.70	22.40	6.75	15.10	2.69	2.62	1.46	8.25	2.81	0.49	3.64	Quartz, calcite, arcanite, sylvite	[5]
BFA	Olive tree and forest, Jaén, Spain	-	-	9.99	22.08	6.65	34.54	4.77	3.64	1.91	7.99	2.33	0.43	2.08	Quartz, calcite, aluminosilicate, sylvite	[81]
BBA	Driftwood waste from biofuel	-	2.68	12.24	4.45	1.85	48.83	6.62	5.32	0.46	10.42	2.45	0.49	3.97	-	[82]
BWA	Wood chips from deciduous trees Arłamów, Poland	-	-	-	17.50	5.16	10.99	1.56	1.48	-	17.22	-	0.43	1.01	-	[83]
Maximum	Maximal value	13.84	3.05	74.31	46.10	14.80	61.00	8.70	8.05	1.91	17.22	5.05	45.72	33.20	-	-
Minimum	Minimal value	0.10	0.68	2.66	0.98	1.07	4.60	1.36	1.19	0.09	1.42	0.85	0.21	0.77	-	-
Mean value	Mean value	1.92	2.29	21.01	18.82	5.89	31.48	4.39	3.61	0.84	6.80	2.47	6.50	8.68	-	-

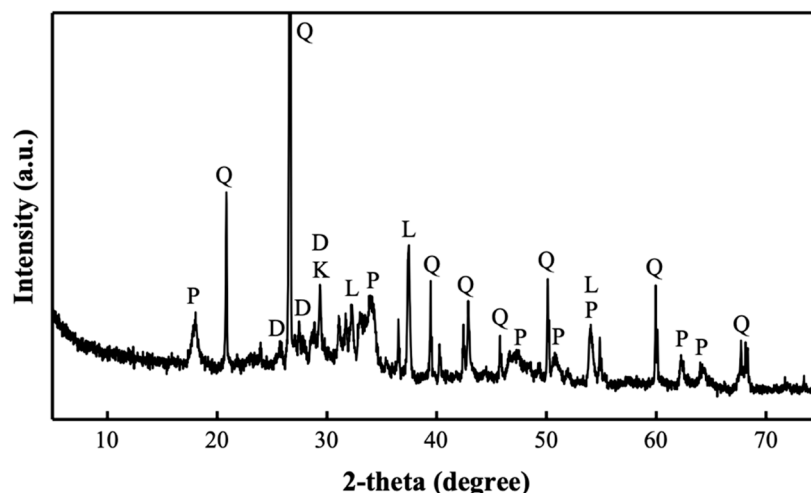


**Figure 3.** XRD pattern of a BWA from pine chip combustion in Vilnius, Lithuania [61] (Q: quartz; D: dicalcium silicate; P: portlandite; L: lime; K: calcite).

The chemical compound of BWA is strongly associated with the burning procedure. Usually, the temperature of wood combustion ranges from 538 to 1093 °C. According to Etiégni and Campbell [85], the wood ash produced from combustion is highly alkaline, and along with the increment in burning temperature, the elemental contents of Ca, iron (Fe), magnesium (Mg), and phosphorus (P) increase, whereas the amount of zinc (Zn), K, and Na decrease. Meanwhile, the alkalinity of BWA is determined due to the contents of hydroxide, carbonate, and bicarbonate in the ash [44]. In Table 1, the chemical composition of BWA differs; nonetheless, the primary oxides are SiO<sub>2</sub>, Al<sub>2</sub>O<sub>3</sub>, or CaO. The highest content of SiO<sub>2</sub> is reported in the BWA from the forest biomass, with 46.10% [58]. The BWA from Portugal has the greatest Al<sub>2</sub>O<sub>3</sub> content of 14.80% [64], while the highest CaO content (61.00%) is recorded in the BWA from timber burning [77].

So as to further compare the chemical composition of diverse BWAs, the distribution of the contents of the principal oxides (SiO<sub>2</sub>, Al<sub>2</sub>O<sub>3</sub>, or CaO), as well as the CaO/SiO<sub>2</sub> ratio and the ratio of basic oxides (MgO, Al<sub>2</sub>O<sub>3</sub>, and CaO) to acidic oxide (SiO<sub>2</sub>), which presents hydraulic properties [86,87], are illustrated in Figure 4. The distribution of the chemical contents exhibits a scattered pattern, indicating a large difference in the characteristics of BWA depending on the source of the biomass and the combustion sets, which explains the great difference between BWA-based AAMs and also enhances the difficulty of establishing a uniform standard of BWA application in AAMs. For most of the ashes, the amount of SiO<sub>2</sub> is less than 30%, while there are several investigations reporting higher SiO<sub>2</sub> content [58,64,79]. The oxide content of Al<sub>2</sub>O<sub>3</sub> is presented as less than 20% for all ashes. It demonstrates that, differently from precursor materials like MK composed of Si and Al, most of the BWA belongs to high-Ca precursors comprised of mainly Si and Ca [88]. In particular, half of the reviewed ashes have a CaO content of over 40% [65,71–73,75–78,82].

The ratio of SiO<sub>2</sub> and CaO is used to characterise the hydraulic activity of materials, which affects their capability to set, harden, and generate hydrates during the reaction with water, further influencing the development of the mechanical properties of the matrices, especially for the high-Ca-content materials [61,89]. According to Lee and van Deventer [90], Ca and Mg compounds in AAMs can help to shorten the initial setting time by providing extra heterogeneous nucleation centres. Puligilla and Mondal [91] also pointed out that the presence of Ca prolonged the dissolution of aluminosilicates in precursor materials, considerably impacting the early- and late-stage behaviours of the hardened binder. For most of the reviewed ashes, the CaO/SiO<sub>2</sub> ratio is recorded as less than two, which fails to meet the required amount for hydraulic materials (CaO/SiO<sub>2</sub> > 2) according to BSEN197-1:2011 standard. Only a few investigations report BWA with a CaO/SiO<sub>2</sub> ratio higher than 10 [65,71,77,78]. The presence of Si and Al compounds in precursors is intensively

connected with the development of hardened strength [92]. In Figure 4, the ratio of basic oxides to acidic oxides centres mainly in the region of less than five. Only a few ashes report a value over 10 [65,71,77,78,82]. These data explain the importance of incorporating more active precursor materials to improve the hydraulic capacity and mechanical properties of BWA-based AAMs.

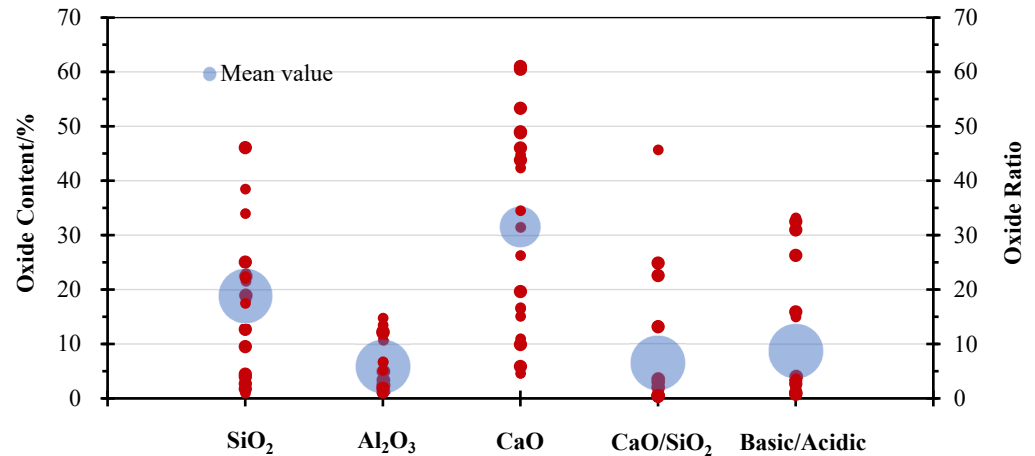


Figure 4. Distribution of the oxide compounds and oxide ratios.

In order to improve the reactivity of BWA, pre-treatment approaches are adopted by researchers, among which decreasing the particle size of ashes via ball-milling is the most common method [38,58,70,71]. In some research, before grinding, 64.5 °C heating treatment for 24 h and sieving through 500 µm sieve are also adopted to enhance the effectiveness of pre-processing [5,93]. Ates et al. [71] compared the chemical-physical properties of treated and untreated BWA, reporting that the ball-milling method greatly improved the specific gravity and specific surface area. The milled BWA had finer and more amorphous particles with fewer micro-cracks between them. Teker Ercaan et al. [5] also pointed out that after being subjected to 10- and 20-min grinding, the mean particle size of BWA was reduced from 18.31 to 3.79 and 4.22 µm, respectively, and 10-min grinding was more effective in modifying the particle shapes and morphology. This can be attributed to the coverage of smaller particles on grinding balls, reducing the efficiency of the milling process, and the wearing out of milling media can negatively impact grinding kinetics [55,94]. The same outcomes were observed by Kumar and Kumar [95] and Hamzaoui et al. [96], indicating that long-time milling can cause agglomeration and deteriorate the microstructure of ashes. Recalcination is another effective pre-processing method which can greatly alter the mineralogical and chemical composition of BWA, increasing the chemical reactivity [71]. But compared to ball-milling, recalcination is less eco-efficient in terms of energy consumption [97].

### 3. Preparation of Alkali-Activated Composites

Table 2 illustrates the mix design and sample preparation of BWA-based AAMs in the highly related investigations from 2019 to 2023, including the type of precursors, utilised alkali solutions, and curing conditions. Most of the research still focuses on the development of alkali-activated paste, without the introduction of aggregates. The studies on mortar and concrete materials are comparably limited, especially the latter, only consisting of less than 10% of the investigations. In the research conducted by Lin et al. [76], alkali activation was also used to produce BWA-based lightweight aggregates, which provide a reference for broadening the application of BWA in AAMs. Regarding the testing methods, in most of the research, compressive and flexural strength were tested, together with the microstructural analysis such as XRD, Fourier transform infrared spectra (FTIR), scanning electron microscopy-energy dispersive X-ray spectroscopy (SEM-EDS), and thermogravimetry (TG). There was little attention paid to the durability, thermal properties, or environmental impacts.

In terms of the alkali activators employed, besides several investigations reporting the application of KOH,  $K_2SiO_3$ , and  $Na_2CO_3$  [5,38,58,71], NaOH and  $Na_2SiO_3$  remain the predominant activators in the majority of research due to their remarkable activating effectiveness. The activation potential of alkali activators can be arranged as  $Na_2SiO_3 > NaOH > NaOH + Na_2CO_3 > KOH$  [98]. Notwithstanding this, the drawback of using Na-based activators is that the production of commercial alkaline activators with Na is associated with intensive energy consumption and a large amount of  $CO_2$  emissions. The manufacturing per kg of NaOH product accounts for the emission of 1.915 kg of  $CO_2$ , and approximately 1.514 kg of  $CO_2$  is generated by the production of 1 kg  $Na_2SiO_3$  [11,99,100]. Also, there is a problem regarding the pollutant aspect due to the high pH and chemical toxicity of NaOH and  $Na_2SiO_3$  [99,101].

KOH and  $K_2SiO_3$  are usually employed to replace NaOH and  $Na_2SiO_3$ . The larger potassium cation ( $K^+$ ) size enables a higher rate of dissolution as well as solubilisation of polymeric ionisation, facilitating the formation of a geopolymer network and larger oligomers, accounting for a higher extent of polycondensation and benefiting the development of mechanical strength [102–104]. In addition,  $K^+$  can enhance the refractory characteristics of AAB and thus provide increasing resistance when exposed to high temperatures [105]. Nevertheless, the challenge associated with the application of KOH and  $K_2SiO_3$  as activators also stems from their elevated alkalinity, presenting significant environmental concerns. To address this issue,  $Na_2CO_3$  is introduced to replace NaOH for producing more sustainable activator solutions. The use of  $Na_2CO_3$  can create a less alkaline environment in the AAMs system and, due to its lower costs, the economic viability of the produced material is greatly improved [38,106,107]. The only limitation is the extended setting time and restricted strength development [108,109].  $Ca(OH)_2$  is another activator option. It is five to six times lower in price compared to NaOH [101], and effective in accelerating the activation process in AAM systems and promoting the formation of CASH, leading to a dense binder microstructure and improving mechanical strength [13,14]. Yet, its application in BWA-based AAMs is still not reported.

As the fundamental ingredients in the fabrication of AAMs, precursor materials significantly affect the mechanical performance and durability of AAMs. Most BWA is of low reactivity, therefore, due to the purpose of guaranteeing the engineering properties of AAMs; they are usually only used as a partial replacement for other more active precursors as binary or ternary binder material, such as metakaolin (MK), FA, and slag-based industrial wastes. The results testify to the positive effects of incorporating BWA as a precursor source to enhance the mechanical properties and improve the microstructure of AAMs at a low replacement ratio; nevertheless, when the content of BWA surpasses 50%, a reduction in the mechanical strength is observed [70,71,77,81]. Phosphogypsum (PG) is an effective source of Ca, preferred in recent years by researchers to be used together as a binary precursor with BWA. Vaičiukynienė et al. [72] and Zhu et al. [38] investigated the influence of the PG replacement ratio on BBA- and BFA-based AAMs, respectively, confirming that the optimal ratio of adding PG was less than 30%. Comparing the different precursors used together with BWA, FA and slags exhibit increasingly remarkable results in improving the mechanical strength and microstructure of BWA-based AAMs, outperforming other materials such as PG or zeolite waste. This can be related to the rich Al and Si contents in them, favouring polycondensation and facilitating alkali activation. Nonetheless, further investigations should be conducted to provide a clearer comparison under the same experimental settings. In addition, it is worth mentioning that, unlike CBMs, the utilisation of reinforcing additives, such as nano-admixtures and fibres, is less universally investigated in BWA-based AAMs, and attention is still being paid to the incorporation of more active precursors.

**Table 2.** Experimental design and preparation of AAMs.

Category	Precursor	Alkali Activator	Testing Methods	Temperature Treatment	Curing Humidity	Major Outcomes	Reference
Paste	BWA, BSS	KOH, K <sub>2</sub> SiO <sub>3</sub>	Compressive strength, flexural strength, FTIR, bulk density, XRD, thermal conductivity, SEM-EDS	60 or 20 °C for 24 h	90%	Thermal curing at 60 °C increased mechanical properties at early curing ages. The addition of up to 50 wt% of BSS contributed to increased compressive and flexural strengths.	[58]
Paste	BWA, FA, GGBS	NaOH, Na <sub>2</sub> SiO <sub>3</sub>	Compressive strength, workability, ultrasonic pulse velocity (UPV), XRD, TG, FTIR, SEM-EDS	Room temperature	65%	Replacement of 30 wt% BWA significantly improved compressive strength and microstructure compared to the reference mixture.	[70]
Paste	MK, BWA	NaOH, Na <sub>2</sub> SiO <sub>3</sub>	Rheological tests, isothermal calorimetry, FTIR, greenhouse gas emissions	-	-	The specific surface area of BWA greatly influenced the rheological parameters and the hydration kinetics of the geopolymers, and BWA had 65% less CO <sub>2</sub> emissions than MK.	[27]
Mortar	FA, BWA	KOH, Na <sub>2</sub> SiO <sub>3</sub>	MIP, compressive strength, flexural strength, XRD, TG, SEM	70 °C for 24 h	-	The inclusion of treated BWA enhanced compressive and flexural strength. The control mix and treated BWA specimens displayed better porosity.	[71]
Paste, concrete	BWA, PG	NaOH, Na <sub>2</sub> SiO <sub>3</sub>	Compressive strength, flexural strength, SEM, XRD, total porosity	60 °C for 24 h	-	15–20% PG replacement led to improved compressive strength. NaOH/Na <sub>2</sub> SiO <sub>3</sub> as activator solution resulted in reduced open porosity and improved samples' resistance to freezing and thawing.	[72]
Paste	BWA, zeolitic waste	NaOH	Compressive strength, XRD, FTIR, SEM	60 °C for 24 h	-	3% zeolitic waste replacement.	[73]
Paste, mortar	BWA, silica fume	NaOH	XRD, SEM-EDS, FTIR, compressive strength, total porosity, Methylene blue concentration reduction	24 °C	50–60%	The alkaline activation of pastes and mortars with 5 M solution exhibited the best levels of compressive strength. Alkaline-activated mortars presented lower water absorption than mortars without activation.	[65]
Paste	BWA, glass powder (GP)	NaOH	Compressive strength, flexural strength, XRD, SEM-EDS,	Room temperature	-	With the increase in NaOH content and reduction in GP, both compressive and flexural strength grew.	[75]

Table 2. Cont.

Category	Precursor	Alkali Activator	Testing Methods	Temperature Treatment	Curing Humidity	Major Outcomes	Reference
Paste	BWA, PG	Na <sub>2</sub> CO <sub>3</sub> , Na <sub>2</sub> SiO <sub>3</sub>	Setting time, density, UPV, compressive strength, water absorption, TG, XRD, SEM	20 and 40 °C	-	The mechanical properties increased with the increase in temperature and Na <sub>2</sub> CO <sub>3</sub> /Na <sub>2</sub> SiO <sub>3</sub> ratio.	[61]
Paste, mortar	BWA, MK	NaOH, Na <sub>2</sub> SiO <sub>3</sub>	XRD, SEM-EDS, workability, bulk density, water absorption, compressive strength	Room temperature	65% for 24 h	Binder/aggregate ratio influenced the properties of the mortar. With an increasing number of aggregates, the compressive strength decreased. Incorporation of BWA up to 20% increased the early strength due to the formation of CSH gel. Only the mortar with 10% BWA replacement showed positive 28-day results.	[64]
Mortar	BWA, FA	NaOH, Na <sub>2</sub> SiO <sub>3</sub>	Compressive strength, flexural strength, water absorption, total porosity, XRD, SEM	70 °C for 24 h	-	Samples obtained with hydrothermal conditions and SS:SH = 1.0 can be used for pollutant adsorption and those produced at room condition with SS:SH = 1.5 can be employed as dense mortars.	[77]
Paste	BWA, MK	NaOH, Na <sub>2</sub> SiO <sub>3</sub>	XRD, TG, SEM-EDS, compressive strength, bulk density, water absorption	40, 20 °C and room temperature	65%, submerged in water and open condition	By increasing the content of GGBS from 0% to 30%, the crushing strength improved from 0.84 MPa to 2.25 MPa, and the water absorption decreased from 24.0% to 12.5%.	[79]
Aggregate	BWA, GGBS	Na <sub>2</sub> SiO <sub>3</sub>	Bulk density, water absorption, crushing strength, pore distribution, XRD, EDS	30 °C	65%	BWA and calcined clays improved the mechanical properties of geopolymer.	[76]
Paste	BWA, MK, calcined clay	NaOH, Na <sub>2</sub> SiO <sub>3</sub>	Bulk density, apparent porosity, water absorption, compressive strength, thermal conductivity, XRD, FTIR, SEM-EDS	60 °C for 24 h	-	Grinding wood ash can improve the mechanical properties of alkali-activated systems compared to untreated wood ash, and the incorporation of wood ash increased the porosity of the binder matrix.	[80]
Mortar	BWA, GGBFS	NaOH, Na <sub>2</sub> SiO <sub>3</sub> , Na <sub>2</sub> CO <sub>3</sub>	Workability, compressive strength, flexural strength, SEM, total porosity, EDS, XRD, pH value, isothermal calorimetry	Room temperature	-	The compressive strength of AAB specimens relied on the amounts of silica gel by-product and alkali activator. The highest strength (21.6 MPa) was observed in specimens with 35% of silica gel by-product.	[5]
Paste	BWA, silica gel by-product	NaOH	Compressive strength, XRD, FTIR, SEM	60 °C for 24 h	-	Concentration of at least 8 M NaOH is required to obtain optimum mechanical properties and up to 50 wt% addition of BWA increased compressive strength.	[74]
Paste	BWA, MK	NaOH, Na <sub>2</sub> SiO <sub>3</sub>	XRD, FTIR, SEM-EDS, bulk density, apparent porosity, water absorption, compressive strength	60 °C for 24 h	-		[81]

Table 2. Cont.

Category	Precursor	Alkali Activator	Testing Methods	Temperature Treatment	Curing Humidity	Major Outcomes	Reference
Mortar	FA, BWA	NaOH, Na <sub>2</sub> SiO <sub>3</sub>	SEM-EDS, FTIR, catalytic tests, metal sorption	Room temperature	-	Geopolymers possess optical and photocatalytic properties. Geopolymers based on BWA had better sorption properties.	[83]
Paste, mortar	BWA, MK	NaOH, Na <sub>2</sub> SiO <sub>3</sub>	Workability, compressive strength, XRD, TG, SEM-EDS	60 °C for 48 h then at 60 °C	RH 95%	Incorporation of MK improved mechanical properties. The highest compressive strength was obtained for 40% MK incorporated mortars for around 38 MPa.	[110]
Paste, mortar, concrete	FA, BWA	NaOH, Na <sub>2</sub> SiO <sub>3</sub>	Setting time, workability, bulk density, flexural strength, sulphate resistance, freeze-thaw resistance	Room temperature	-	The mixtures with 20% BWA showed better sulphate resistance than those with only FA.	[82]

Curing condition is another crucial factor influencing the properties of AAMs, especially temperature treatment, which can help the dissolution of minerals in precursors and facilitate the process of alkali activation [111,112]. Particularly at the early stage, being subjected to heating can improve early strength development and reduce the setting time of AAMs [113,114]. As is shown in Table 2, most researchers adopted the temperature treatment at 60 °C for 24 h, then transferred the samples to room temperature for the rest of the curing period, also due to the consideration of controlling environmental and economic impacts. Curing at 50 °C per 24 h can lead to an increment in CO<sub>2</sub> emission by 11% [100]. In the research conducted by Gómez-Casero et al. [58] and Zhu et al. [61], which compared the properties of AAMs with or without heating, their outcomes confirmed the positive effects of temperature treatment. However, to thoroughly indicate the effectiveness of temperature curing, a systematic analysis involving both engineering performance and environmental assessment is still needed.

#### 4. Properties of Alkali-Activated Composites Containing Biomass Wood Ash

##### 4.1. Workability and Setting Time

As is indicated in the literature, there is a consensus that when the BWA ratio in the blended binder increases, the workability exhibits a significant downtrend [5,70,77,110]. Tran Thi et al. [70] pointed out that as the incorporation of BWA content increased (from 30 to 50 to 70%) to replace the GGBFS and FA mixture, the flowability of paste samples experienced a reduction in the range of 13.8–27.9%, 30.5–40%, and 36.7–43.2%, respectively. They ascribed it to the great LOI and porosity of BWA, requiring more free water and thus decreasing the flowability. Another reason could be the high specific surface area of BWA and its irregular particle shape, which exerts an adverse influence on the workability [77]. A different tendency was reported by Bijeljić et al. [82] who observed the growing flowability of mortar mixtures from 122 mm to 141 mm when FA was replaced by BWA from 0 to 25%. They explained that the particle size of FA was finer than 0.1 mm, requiring a larger amount of water, thus when the ratio of FA decreased, the workability correspondingly improved.

In terms of setting time, existing investigations report that by enhancing the BWA content in the binder, both initial and final setting time are remarkably shortened [70,77,82]. Abdulkareem et al. [77] observed an initial setting time decreasing from 210 min to 120 and 35 min when the amount of BWA increased from 10 to 20 and 30%, respectively. This is associated with the high calcium content in most of the BWA contributing to fast setting [82,115]. The water from the alkali solutions undergoes a reaction with certain calcium compounds from BWA, such as portlandite, resulting in the formation of calcium silicate hydrate (CSH) gels which enhance the alkalinity of the solution and contribute to increased setting rates [116].

The growing SiO<sub>2</sub>/Na<sub>2</sub>O ratio in the alkali activator solutions, on the contrary, can enhance both the flowability and setting time of AAMs. Tran Thi et al. [70] aligned this to the highly polymerised silicate ions which hinder the setting. In addition, when the SiO<sub>2</sub>/Na<sub>2</sub>O ratio increases, the coating on the precursor particle surface is improved, which reduces the rolling friction between the particles, enhancing flowability [117]. The workability of AAMs with BWA follows the ranking order of Na<sub>2</sub>SiO<sub>3</sub> > Na<sub>2</sub>CO<sub>3</sub> > NaOH [5]. Similar results are demonstrated by Zhu et al. [61], who investigated the effects of the Na<sub>2</sub>CO<sub>3</sub>/Na<sub>2</sub>SiO<sub>3</sub> ratio, highlighting a significantly shortened final and initial setting time due to the improvement of Na<sub>2</sub>CO<sub>3</sub> content. This is owing to the growing calcium ions dissolved and precipitated with carbanions, speeding up the setting [118].

##### 4.2. Mechanical Properties

Compressive strength is one of the most significant engineering properties for assessing the application of new building and construction materials. The mechanical strength of AAMs is associated with the densification of the materials and is also attributed to the cementitious products formed during the process of hydration and alkali activation. Due

to the low reactivity of BWA, the AAMs with 100% BWA possess a strength value within the range between 8.5 and 22.0 MPa, heavily depending on the chemical and mineralogical composition of the ash [38,58,72,73,81]. Therefore, to ensure the quality of fabricated AAMs, most researchers apply binary or ternary precursors to be incorporated together with BWA. These precursor materials usually have a greater reactivity and can effectively facilitate the development of alkaline aluminosilicate gel or geopolymer gel in the binder system. The most commonly added materials include the industrial by-product FA from coal burning, slags, and MK. Abdulkareem et al. [77] pointed out that the replacement of FA with 10% high-calcium BWA contributed to a 106% strength increment compared to the mortar with only FA. This can be related to the increased degree of alkali activation and the secondary hydration of CaO from BWA reacting with silicate and aluminate to form CSH and CASH gels, which fill the voids as micro-aggregates and generate a denser binder structure [119,120]. By adding 50% black steel slag (BSS) and 50% BWA as precursors, Gómez-Casero et al. [58] reported an 86.8% increment of compressive strength from 22.0 to 41.1 MPa. Unlike BWA particles, the dissolution of the glassy phase of BSS is comparatively less dependent on the breakage of Si–O–Si by Si–O–Al bonds, which facilitates the alkali reactions after its addition [121]. In the case of MK, when 50% MK and 50% BWA are used together, a greater strength of 44.0 MPa is achieved, while the single incorporation of BWA or MK only contributes to a strength value of 18.1 and 23.0 MPa, respectively [81]. However, when the ratio of BWA is high, the strength loss is observed owing to the growing organic content in the matrix, which limits the polycondensation and enhances setting time [122]. In other investigations, the binary usage of BWA and 40, 50, and 60% replacement with silica fume contributed to the 28-day compressive strength above 55 MPa [65]. The introduction of glass powder at 30% binder weight led to an increment of 14-day strength value from 2.96 to 19.62 MPa compared to the sample with 100% BWA [75]. And the combination of 3% waste zeolite enhanced the 28-day compressive strength from 8.5 to 14.7 MPa [73].

Several factors influence the development of compressive strength of AAMs. Temperature treatment is reported as favourable for achieving better compressive behaviours. After elevating the curing temperature from 20 to 60 °C, the 28-day compressive strength of alkali-activated paste with only BWA improved from 13.8 to 22.0 MPa, which can be ascribed to the increased dissolution degree of reactive contents in the solid precursors, such as Al, Ca, and Fe species, accelerating the reaction rate and accounting for greater polycondensation and polymerisation [58]. Conversely, heat treatment can have disadvantages, too, especially in the long term, when the degree reaction stays approximately the same, but due to the faster hardening process, less ordered and poorer quality microstructures are formed [123]. The grinding processing of BWA in advance also favours the development of strength. According to Teker Ercan et al. [5], after the milling treatment, strength can be improved by up to 39.81%. This is primarily because of the high unburnt carbon content and unreactive wood residue particles hindering the alkali activation of BWA [69]. In terms of the effects of alkali activators, Silva et al. [65] concluded that the use of 5 M NaOH solution outperformed 10 and 15 M in the development of compressive strength, due to the excessive number of alkaline ions disabling the condensation of Si and Ca ions to form the gels. Similar results were obtained by Silva et al. [75], who showed that when the NaOH concentration was elevated from 2 to 5 M, the compressive strength of AAMs with only BWA decreased from 2.96 to 3.69 MPa. Compared to NaOH and Na<sub>2</sub>CO<sub>3</sub> solutions, higher compressive strength is achieved when Na<sub>2</sub>SiO<sub>3</sub> is used as an activator [5]. It can be connected to improved polycondensation when the activating solution contains Na<sub>2</sub>SiO<sub>3</sub>, which provides the Si species available in the solution [124].

#### 4.3. Durability

In the currently existing studies regarding BWA-based AAMs, the primary focus has been on water absorption and the other durability properties are rarely involved. Generally, the influence of BWA on AAMs varies, associated with the other incorporated

precursors. Jurado-Contreras et al. [81] demonstrated that the substitution of MK with BWA contributed to the decrease in water absorption values from 34 to 33–12% and, along with the enhancement of the BWA ratio, the water absorption exhibited a reduction. They ascribed it to the formation of a denser structure of the paste, with BWA serving as a filler to fill the spaces, voids, and pores. The same results were obtained by Eliche-Quesada et al. [80], highlighting that the use of BWA to partially replace MK accounted for a more compact structure and reduced water absorption values. Different outcomes were reported when FA or PG were used together with BWA [61,77]. By increasing the content of BWA, the insufficient geopolymerisation reaction contributed to low compactness and was sustained by higher 28-day water absorption [77]. Another reason can be attributed to the great amount of unburnt carbonised organic matter in BWA, actively absorbing water owing to its highly porous structure [125,126].

Concerning the influence of alkali activators, the decrease in NaOH concentration leads to lower water absorption values [81]. Similar outcomes were observed by De Rossi et al. [79], who showed that when decreasing the  $\text{Na}_2\text{SiO}_3/\text{NaOH}$  ratio from 1.5 to 1.0, greater values of water absorption were observed. This is due to the increased amount of free water available in the paste system, which results in higher fluidity and porosity, as well as lower paste consolidation.

#### 4.4. Bulk Density

The bulk density of the produced AAMs containing BWA is connected to the density of additional binary precursors, the type of alkali solutions, and the curing environment. As is interpreted in some investigations [80–82], the incorporation of BWA can improve the bulk density of AAMs, not only due to the density of BWA but also the filling and type of gel enrichment effects of BWA, which can lead to a more densified structure. Gómez-Casero et al. [58] demonstrated an uptrend of bulk density growth along with the increasing curing temperature and age. The enhanced thermal curing at 60 °C can facilitate the dissolution of reactive precursor phases, fostering a more substantial reaction. This process reduces the number of voids in the matrix, leading to a higher volume of gel and densification [127]. While extending the curing duration promotes the extended structure of hydration products, diminishing porosity through improved cohesion and adhesion among matrix components ultimately results in densification. A different tendency was revealed by Zhu et al. [61], with a reduction in density observed when the curing temperature was elevated to 40 °C. The distinguishment in the results may be associated with the different curing humidity. In the case of the latter, no humidity control was applied; thus, the evaporation of free water could be accelerated when samples were subjected to temperature treatment. In hydrothermal situations, the promotion of the new phase generation is sustained with the densification process and thus the enhancement of bulk density [128]. They suggested improving the  $\text{Na}_2\text{CO}_3/\text{Na}_2\text{SiO}_3$  ratio to facilitate the new phase formation and prevent water evaporation. Similarly, when the  $\text{Na}_2\text{SiO}_3/\text{NaOH}$  ratio was enhanced from 1.0 to 1.5, the bulk density of AAMs was raised due to an elevated quantity of  $\text{Na}_2\text{SiO}_3$ , which augmented the viscosity of the alkaline solution, elevating the compactness of the network structures [79,129].

#### 4.5. Phase Identification

Based on the XRD identification, the major crystalline components detected in the BWA-based AAMs are quartz and calcite [5,81,110], which are also the elemental mineralogical components in BWA raw materials. This indicates that these crystalline phases in BWA are inactive particles and can perform as filler particles in AAMs [124,130]. The alkali activation of BWA leads to the newly formed crystalline compounds in AAMs, including CSH, CASH, and sodium aluminosilicate hydrates (NASH) [71,74]. When the concentration of the alkali solution increases, the peaks of the newly formed phases are more intensive, interpreting increasingly intense alkali activation [65]. In contrast with the patterns belonging to the precursors, Jurado-Contreras et al. [81] observed shifts in

the peaks of alkali-activated bricks towards higher  $2\theta$  degree, indicating the formation of amorphous NASH gel in the matrix [114,131,132]. The intensity of this amorphous halo decreased with the growing content of BWA, testifying to the higher degrees of polycondensation. Also, some studies reported the formation of amorphous phases of CASH and CSH gel in the range of  $20\text{--}38^\circ$ , which is significantly connected with the development of mechanical strength [75,110,133–135]. When the BWA is rich in calcite, there can be also the hydrotalcite (Ht)-like phase generated during alkali activation, which presents more intense and sharper peaks with the increment of BWA contents [70,136]. In BWA, calcite may undergo partial dissolution under alkaline conditions, leading to the release of increased  $\text{CO}_3^{2-}$  and promoting the formation of more Ht-like phases [137,138]. Another point worth noting is that the curing temperature shows limited impact on the transformation of crystalline phases in the precursors, and structural changes primarily occur in the amorphous phase, but curing at a moderate temperature of  $60^\circ\text{C}$  can contribute to a more pronounced surface attack on the crystalline phases, releasing reactive silica and facilitating gel formation, which favours the early-age strength development [58,139].

In the thermogravimetry-derivative thermogravimetry (TG-DTG) and thermogravimetry-differential thermal analysis (TG-DTA) curves, the primary weight loss occurs from  $80$  to  $800^\circ\text{C}$ . The mass loss of hydrated AAMs at the temperature from  $80$  to  $250^\circ\text{C}$  corresponds to the evaporation of free and physically bound water [79], decomposition of CSH [61,140], as well as NASH, which showed an increasing amount along with the decline of BWA content [110]. The water loss from portlandite formed in the pastes due to the hydration of lime. The dehydration of unburnt organic matter in BWA and the decomposition of Ht-like phases occur at  $300\text{--}500^\circ\text{C}$ , while the weight loss owing to the decomposition of calcite is in the temperature range above  $500^\circ\text{C}$  [57,61,110,138].

Along with the increase in BWA content, in the FTIR spectra, the intensity of the functional bands assigned to  $\text{--OH}$  stretching and the  $\text{H--O--H}$  bending vibrations from bound water molecules exhibit a reduction, interpreting lower adsorption of water and less gel formation in the AAMs [81,141]. The increasing intensity of  $\text{O--C--O}$  vibration in the carbonate phases between  $1450$  and  $870\text{ cm}^{-1}$  can be associated with the high carbonate content in BWA [142,143], or the reaction of the alkali-activated binder with  $\text{CO}_2$  from the air in the environment [27,144]. The alkali activation of BWA leads to the generation of new amorphous phases in AAMs, especially NASH gel, contributing to the shift of  $\text{Si--O--Si/Al}$  bands, which is more remarkable when the concentration of alkali solutions is improved [80,81,145,146]. The shift of the peaks is also more pronounced when the samples are subjected to the temperature treatment which favours the dissolution of precursors and accelerates alkali activation, leading to the production of a larger amount of gel [58,147]. In a more alkaline environment, the degree of alkali activation reaction is improved owing to the dissolution of a larger number of precursors, accounting for the increasingly common substitution of  $\text{Si--O}$  or  $\text{Si--O--Si}$  with  $\text{Si--O--Al}$  at the tetrahedral sites, which provides more nucleation sites within the three-dimensional matrix structure and results in a localised alteration of the  $\text{Si--O}$  bond [148,149].

#### 4.6. Microstructure and Porosity

When 100% BWA is used as a single precursor material, the poorly dissolved BWA particles contribute to a porous and less compacted gel-like microstructure of the AAM matrix, without interconnection between the particles, which adversely influences the development of mechanical strength [110]. This is associated with the growing void volume of the structure owing to the porous nature of BWA as well as the great number of un-hydrated BWA particles [70]. The shrinkage between the unreacted particles leads to the propagation of micro-cracks and agglomerated products precipitated on the particle surface, responsible for the microstructural defects and negatively affecting the compressive strength [77,81]. Another reason could be that the addition of BWA reduces the formation of denser CASH gel via promoting the generation of high-porosity NASH gel [150]. After adding a binary precursor, BWA particles are well embedded and connected to the matrix,

leading to a denser morphology of AAMs [110]. Meanwhile, the filling effect of BWA in the voids and pores gives rise to increasing densification of the hybrid binder [80]. Alkali activator solutions tremendously influence the dissolution and reaction degree of BWA during the alkali activation. The increment of activator concentration is usually linked to a more condensed morphology. A greater activator modulus supplied increased reactive aqueous silica, leading to the formation of more gels, further contributing to refining pores in the hardened pastes and establishing a more homogeneous structure due to the even distribution of the reaction products [151,152]. A more compacted morphology is observed with 60 °C of temperature curing, which promotes the dissolution of aluminosilicates and calcium phases in the precursor, accelerating the formation of the new polymer chain and CSH/CASH gel; however, heat treatment can also introduce micro-cracks into the matrix due to fast evaporation of the water molecules [58].

In the existing literature, the research regarding the pore structure and porosity of AAMs with the inclusion of BWA is still minimal [71,72,77,80,81]. Generally, along with the increasing content of BWA, the total porosity of AAC displays an enhancing tendency due to the highly porous microstructure of BWA [153]. The pre-processing of BWA via grinding can effectively improve the pore structure of BWA-based AAMs and contribute to a smaller average pore diameter due to the effect of treatment, which accounts for finer particle size distribution and more densely packed particles of BWA [71]. Abdulkareem et al. [77] observed a decline in the total porosity of alkali-activated samples with 10 and 20% BWA during the early curing age from three to seven days, with 18 and 15%, respectively. They attributed it to the great degree of alkali activation reaction resulting from the inclusion of up to 20% BWA, which promoted the formation of CSH gel and the refined microstructure of the binder. Concerning the impacts of alkali solutions, the porosity of the AAMs activated by various alkali solutions might be following the order of  $\text{Na}_2\text{CO}_3$  >  $\text{NaOH}$  >  $\text{Na}_2\text{SiO}_3$ -activated samples [5]. The use of  $\text{Na}_2\text{SiO}_3$  solution introduces more active Si into the system, favouring the alkali activation reaction [154]. And the elevated pH values due to  $\text{Na}_2\text{CO}_3$  or  $\text{NaOH}$  solutions facilitate the formation of hydrates, accounting for a denser matrix due to the pore-filling effects [155]. Similar results were obtained by Vaičiukyniene et al. [72], addressing that via replacing  $\text{NaOH}$  solution with  $\text{NaOH}$ - $\text{Na}_2\text{SiO}_3$  solution, a greater quantity of closed pores was formed, and the number of open pores was reduced, which could tremendously improve the durability of alkali-activated concrete.

## 5. Lifecycle Assessment and Analysis of Eco-Efficiency

Wood biomass is widely esteemed as an energy source because of its  $\text{CO}_2$  neutrality, emitting nearly the same amount of  $\text{CO}_2$  during combustion as it absorbs throughout its growth [66,97]. With the increasing application of biomass fuel, the by-product BWA has aroused a significant problem regarding its disposal. The utilisation of BWA in the manufacturing of building and construction materials has the potential to improve eco-efficiency, especially considering the waste management costs and environmental burdens due to landfills. BWA has the capability to capture and mineralise  $\text{CO}_2$  through the hydration process, leading to a remarkable reduction in greenhouse gas emissions from the end product [156,157]. In the domain of cement-based materials with BWA, many investigations have been conducted to evaluate the economic and environmental benefits aligned with the partial replacement of Portland cement (PC) with BWA through the tool of lifecycle assessment, confirming its superiority in reducing manufacturing costs and environmental burdens [97,158–160]. Substituting 40% of PC with BWA resulted in a 32.77% reduction in concrete production costs [158]. And the cost of geopolymer-PC hybrids with BWA was half the price of traditional PC [161]. The only concern lies in the pre-treatment, which significantly enhances the energy demand. Approximately 11.9 kWh/t and 2.2 kWh/t are required for the grinding and sieving process of BWA [159,162]. And if more complex procedures, such as washing, drying, and recalcination, are included, the energy consumption is correspondingly increased [163].

As for BWA-based AAMs, although sustainability and environment conservation due to BWA valorisation have been widely mentioned in the literature, currently, investigations involving environmental or cost analyses are still rare. Only Silvestro et al. [27] calculated the CO<sub>2</sub> emissions of precursors, and per cubic meter manufactured of geopolymer products containing BWA, highlighting that BWA exhibited a decline of almost 65% in greenhouse gas emissions concerning the MK. With regard to a comprehensive lifecycle assessment, however, still no reports have been seen in this field.

## 6. Discussion on the State-of-the-Art Research

Based on the core collection on the Web of Science, Figure 5 summarises the results from a bibliometric search about the trend of publications on the incorporation of BWA in CBMs and AAMs during the time span from 2010 to 2023. Overall, in contrast to the research topics of other types of building materials, the publications on BWA-based materials are still limited and in the beginning stage. From 2010 onwards, the number of investigations reported on BWA in both fields depicts a growing tendency, which can be attributed to the rising attention being given to sustainability in the management of industrial by-products and the increasing worldwide utilisation of biomass-based renewable energy. More interest is observed in CBMs compared to AAMs, which can be ascribed to the universal application of CBMs in engineering practice, and also to the diversity of BWA incorporations, such as supplementary cementitious materials and aggregates [48,164–166]. Nonetheless, owing to rising concerns about the environmental burdens created during the production of Portland cement, the concept of cementless and cement-free binder materials has attracted umbrella interest. This leads to an improvement in the investigations on BWA-based AAMs and geopolymers, especially after 2015, as is observed in the curves, and a tendency to surpass those on CBMs in the year of 2023.

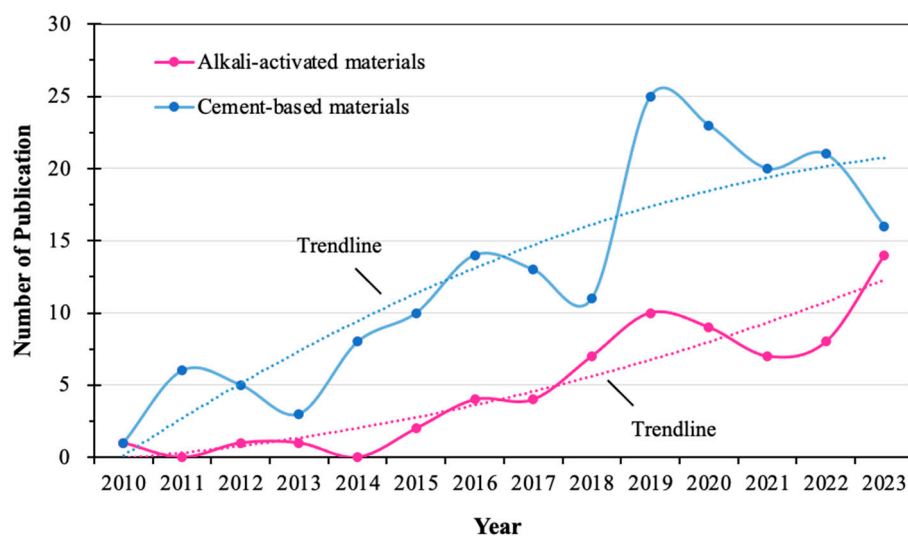


**Figure 5.** Number of publications regarding BWA in the area of CBMs and AAMs.

Figures 6 and 7 illustrate the outcomes of bibliometric analysis based on the refined dataset of 187 highly related publications via the VOSviewer mapping tool. VOSviewer generates a series of networks according to the provided bibliographic data and combines the information in the literature into clusters via a smart local moving algorithm [167,168]. In Figure 6, the co-authorship network of countries is displayed by years using various colours to present the chronological order of the results. Overall, a total number of only 32 countries were defined in the algorithm, with weak cooperation with the research and significant intellectual isolation across different regions observed in the network. Despite a strong link centring in Portugal, most of the countries have no interconnection. There is insufficient international coordination and common policy in the use and application of BWA. This can be associated with the distinguishment of energy policy in different

countries, and for most of the regions where coal is still the main source of energy production, the demand for BWA recycling is less significant. The five leading countries with citations over 100 are Portugal, Germany, Brazil, Thailand, and Spain, and since 2023, several countries have emerged in this research area, which can be related to the rising utilisation of biomass fuel. In total, 255 authors were detected by VOSviewer from the core dataset. After applying the algorithm, 45 authors with a minimum of two documents were chosen, and the result of the co-authorship mapping is illustrated in Figure 7. Similar to the outcomes in the co-authorship network of countries, independence among research groups was observed. Seven collaboration networks of authors were depicted in isolated groups and three single authors were disconnected from the network.

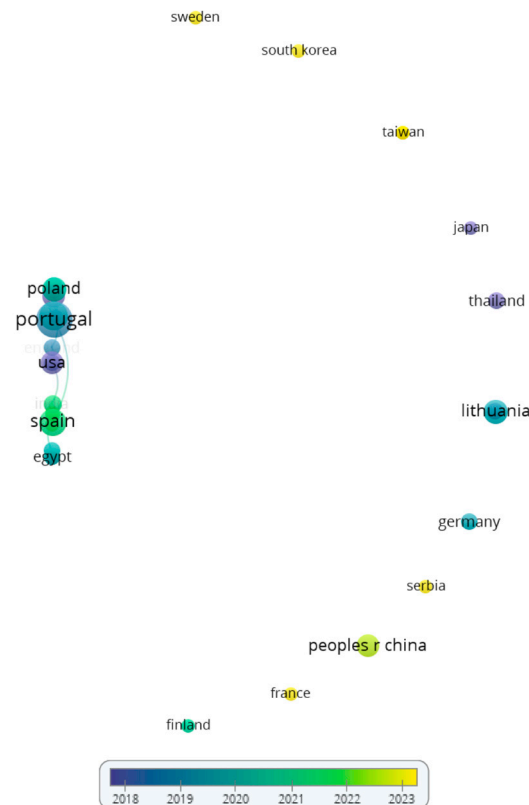


**Figure 6.** Co-authorship network of countries.

Figure 8 exhibits the co-occurrence map of keywords. A total number of 451 keywords was initially identified by VOSviewer and after the refinement to eliminate the generic terms and the terms with the same meaning [169], a network of 394 keywords was illustrated. The occurred keywords can be mainly divided into six groups: (1) treatments and curing conditions of the materials, such as “curing temperature”, “ball milling”, and “grinding”; (2) mix design and the selection of raw materials, like “superplasticizer”, “sodium silicate”, “sodium carbonate”, and “SiO<sub>2</sub>/Na<sub>2</sub>O ratio”; (3) testing of the engineering properties, such as “setting time”, “durability”, “early-strength properties”, “compressive strength”, “workability”, and “freeze-thaw resistance”; (4) incorporation of other by-products—for example, “phosphogypsum”, “fly ash”, “metakaolin”, and “furnace slag”; (5) analysis of microstructure and mechanism, such as “SEM”, “reaction-kinetics”, “hydration”, “porosity”, and “XRD”; (6) sustainability-related analysis—for instance, “CO<sub>2</sub> emissions”, “energy consumption”, “waste valorisation”, and “cost analysis”.



materials, especially the ones with improved compressive strength, via the use of various curing conditions, the incorporation with auxiliary materials of high reactivity, and the introduction of effective activators. Further attention has been paid to investigations on the material microstructure and the reaction mechanism. Along with growing concentration on the development of cement-free eco-binders, the trend then has shifted towards the recent idea of identifying the environmental impacts of the materials, centring on the emission analysis of CO<sub>2</sub> and other greenhouse gases, as well as the production's demand of energy. Meanwhile, the enhancement of durability and economic feasibility has obtained increasing interest. The occurrence of the keyword "circular economy" in 2023 indicates the growing demand in the building and construction industry for facilitating sustainable development and waste management via reducing waste, and maximising the recycling, reuse, and recovery of possible resources [170,171]. The idea of a circular economy advocates for the efficient utilisation of resources and the achievement of zero carbon emissions by transforming end-of-life waste into economic resources, emphasising sustainability in consumption [171–173]. Another point worth noting is the application of optimisation methods and data mining introduced into the investigation, indicating a tendency to combine multi-disciplinary research approaches.

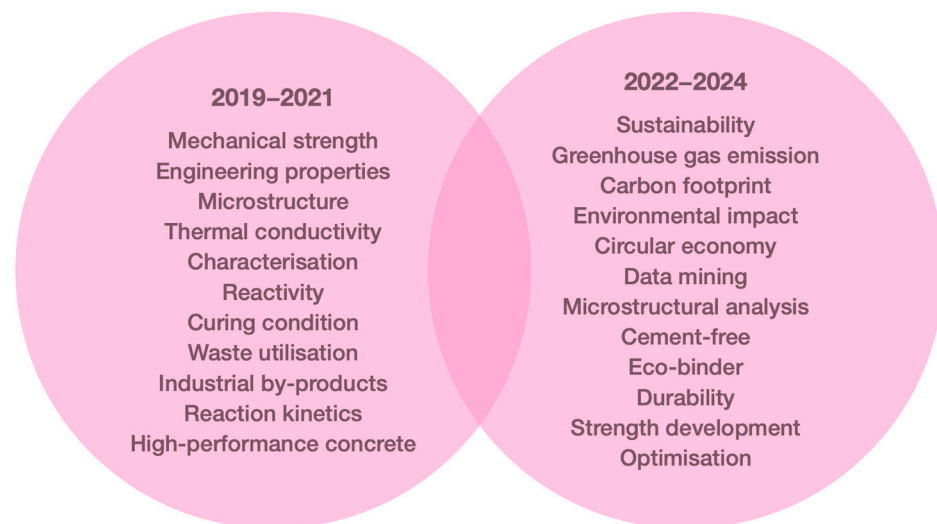


**Figure 9.** Research evolution by years.

## 7. Conclusions and Future Research Perspectives

This review has examined the characteristics and application of BWA in the production of ecological cement-free AAMs. There is great distinguishment in the physical-chemical properties of BWA which heavily depend on the biomass sources and combustion conditions of the power plant. This difference in the raw ashes increases the difficulties and challenges of utilising BWA, especially since the chemical composition plays a crucial role in determining the engineering performance of AAMs. For most of the raw ashes, mineralogical components consist primarily of quartz and calcite, while some of them also contain portlandite and lime. Concerning the chemical composition, most ashes are composed of a comparably high amount of CaO and SiO<sub>2</sub>—up to 46.1 and 61.0%, respectively—and over 70% of them contain Al<sub>2</sub>O<sub>3</sub> at a level less than 6.75%. This determines that they are of low chemical reactivity and hard to dissolve even in a highly alkaline ambient environment. In contrast with the conventional by-products universally applied as precursors to produce AAMs, such as FA, MK, and slags, the hydraulic reactivity of most BWA fails to meet the requirements, limiting strength development when they are incorporated as precursors. The morphology of BWA via SEM shows a porous, non-homogeneous structure with irregularly shaped particles, which is linked with the high porosity of AAM samples if BWA is used in a large ratio. A 10% increment of the amount of BWA in AAMs can account for a 30% increase in the porosity. Another element hindering the evolution of mechanical

strength is attributed to the unburnt wood residues in BWA, particularly the high carbon content, which also leads to a great LOI.

In order to improve the reactivity of BWA, some pre-processing methods are adopted, with the most umbrella one being the ball milling that effectively decreases the particle size distribution of BWA and accounts for a growing homogeneous morphology. Recalcination and washing are also proven to be effective, which, nonetheless, are associated with concerns about enhancing the energy consumption and environmental burdens of AAM production. In the current literature, the investigations are still centred on pastes and mortars, with less focus devoted to the manufacturing of concrete. And the research elementally concentrates on the binary or ternary usage of BWA with other precursor materials (FA, MK, PG, and slag); no attention has been paid to the effects of reinforcing additives, such as fibre and nanomaterials, which have been widely used in CBMs. One possible reason can be attributed to the higher cost of incorporating these additives; however, research is needed to compare their effectiveness. As a binary precursor used together with BWA, materials rich in Al and Si, such as FA and slags, account for more impressive enhancement in the mechanical properties of BWA-based AAMs, in contrast with PG which supplies a source of Ca. However, further research is needed for a thorough investigation. Heat treatment from 30 to 70 °C is also an umbrella method used during the preparation of AAMs. Most researchers adopt 24-h temperature curing in order to improve sustainability and some combine the temperature with controlled humidity to prevent cracks due to the fast evaporation of water.

The most commonly tested properties at present include mechanical strength (especially compressive strength), density evolution, microstructural analysis, and phase-change identification. With regard to durability, except for water absorption, other properties have still not been investigated. Generally, a high ratio of BWA incorporation results in the low strength, high porosity, and inferior structure of AAMs due to the porous nature and low chemical reactivity of BWA. However, a proper content of BWA used together with other precursors exerts a positive influence on the strength development, which can reach even 106%. This is connected with the effect of BWA acting as a micro-aggregate to fill the voids and pores, contributing to a denser structure. Meanwhile, the CaO in BWA can react during the alkali activation to form CSH gel, favouring strength gain. Another point worth mentioning is that although the utilisation of BWA to produce AAMs is always considered a more sustainable alternative binder material for PC, nevertheless a thorough LCA and eco-efficiency analysis on the effects of BWA addition on the environmental and economic feasibility is still lacking. On the other hand, the concepts of a circular economy and optimisation have gradually aroused researchers' attention in recent years.

Despite the promising results in the literature, there is still not enough research on the effects of BWA on AAMs, and the underlying mechanisms are not fully understood. More research should be conducted to figure out the feasibility of incorporating a large quantity of BWA, instead of using it as a partial replacement in a small amount. Besides the development of high-performance BWA-based AAMs, for future investigations, more attention should be paid to the durability properties, particularly the long-term performance in extreme surroundings. In addition to the introduction of binary precursors, the effectiveness of the incorporation of reinforcing admixtures could be investigated. Furthermore, quantitative analysis is needed to understand the sustainability and cost efficiency of the utilisation of BWA. And data mining, as well as multi-criteria optimisation methods, can be adopted for comparing and locating the optimal mixes.

**Author Contributions:** Conceptualisation, Y.D. and I.P.; methodology, Y.D.; software, Y.D.; validation, I.P., J.P., M.K. and A.K.; formal analysis, Y.D., G.G. and I.P.; investigation, Y.D.; resources, M.K., J.P. and G.G.; data curation, Y.D.; writing—original draft preparation, Y.D.; writing—review and editing, I.P. and A.K.; visualisation, Y.D.; supervision, I.P. and A.K. All authors have read and agreed to the published version of the manuscript.

**Funding:** This research was conducted as part of the execution of Project “Mission-driven Implementation of Science and Innovation Programmes” (No. 02-002-P-0001), funded by the Economic Revitalisation and Resilience Enhancement Plan “New Generation Lithuania”.

**Data Availability Statement:** Not applicable.

**Acknowledgments:** The authors offer their sincere gratitude to all the staff in the Institute of Building Materials, Vilnius Gediminas Technical University, and the Institute of Materials and Structures, Riga Technical University for their generous assistance.

**Conflicts of Interest:** The authors declare no conflicts of interest.

## References

- Huntzinger, D.N.; Eatmon, T.D. A Life-Cycle Assessment of Portland Cement Manufacturing: Comparing the Traditional Process with Alternative Technologies. *J. Clean. Prod.* **2009**, *17*, 668–675. [\[CrossRef\]](#)
- Frías, M.; Rodríguez, O.; de Rojas, M.I.S.; Villar-Cociña, E.; Rodrigues, M.S.; Junior, H.S. Advances on the Development of Ternary Cements Elaborated with Biomass Ashes Coming from Different Activation Process. *Constr. Build. Mater.* **2017**, *136*, 73–80. [\[CrossRef\]](#)
- Pierrehumbert, R. There Is No Plan B for Dealing with the Climate Crisis. *Bull. At. Sci.* **2019**, *75*, 215–221. [\[CrossRef\]](#)
- Liu, Z.; Deng, P.; Zhang, Z. Application of Silica-Rich Biomass Ash Solid Waste in Geopolymer Preparation: A Review. *Constr. Build. Mater.* **2022**, *356*, 129142. [\[CrossRef\]](#)
- Ercan, E.E.T.; Cwirzen, A.; Habermehl-Cwirzen, K. The Effects of Partial Replacement of Ground Granulated Blast Furnace Slag by Ground Wood Ash on Alkali-Activated Binder Systems. *Materials* **2023**, *16*, 5347. [\[CrossRef\]](#) [\[PubMed\]](#)
- Pasupathy, K.; Sanjayan, J.; Rajeev, P. Evaluation of Alkalinity Changes and Carbonation of Geopolymer Concrete Exposed to Wetting and Drying. *J. Build. Eng.* **2021**, *35*, 102029. [\[CrossRef\]](#)
- Zhang, Z.; Zhu, Y.; Yang, T.; Li, L.; Zhu, H.; Wang, H. Conversion of Local Industrial Wastes into Greener Cement through Geopolymer Technology: A Case Study of High-Magnesium Nickel Slag. *J. Clean. Prod.* **2017**, *141*, 463–471. [\[CrossRef\]](#)
- Awoyera, P.O.; Adesina, A.; Sivakrishna, A.; Gobinath, R.; Kumar, K.R.; Srinivas, A. Alkali Activated Binders: Challenges and Opportunities. *Mater. Today Proc.* **2020**, *27*, 40–43. [\[CrossRef\]](#)
- Ślosarczyk, A.; Fořt, J.; Klapiszewska, I.; Thomas, M.; Klapiszewski, Ł.; Černý, R. A Literature Review of the Latest Trends and Perspectives Regarding Alkali-Activated Materials in Terms of Sustainable Development. *J. Mater. Res. Technol.* **2023**, *25*, 5394–5425. [\[CrossRef\]](#)
- Patil, P.P.; Katare, V.D. Development of Sustainable Alkali-Activated Binder for Building Products Using Sugarcane Bagasse Ash: A Review. *Mater. Today Proc.* **2023**, *in press*. [\[CrossRef\]](#)
- Mendes, B.C.; Pedroti, L.G.; Vieira, C.M.F.; Marvila, M.; Azevedo, A.R.G.; de Carvalho, J.M.F.; Ribeiro, J.C.L. Application of Eco-Friendly Alternative Activators in Alkali-Activated Materials: A Review. *J. Build. Eng.* **2021**, *35*, 102010. [\[CrossRef\]](#)
- Provis, J.L. Geopolymers and Other Alkali Activated Materials: Why, How, and What? *Mater. Struct.* **2014**, *47*, 11–25. [\[CrossRef\]](#)
- Akturk, B.; Kizilkanat, A.B.; Kabay, N. Effect of Calcium Hydroxide on Fresh State Behavior of Sodium Carbonate Activated Blast Furnace Slag Pastes. *Constr. Build. Mater.* **2019**, *212*, 388–399. [\[CrossRef\]](#)
- Yuan, B.; Yu, Q.L.; Brouwers, H.J.H. Assessing the Chemical Involvement of Limestone Powder in Sodium Carbonate Activated Slag. *Mater. Struct.* **2017**, *50*, 136. [\[CrossRef\]](#)
- Ibrahim, M.; Maslehuddin, M. An Overview of Factors Influencing the Properties of Alkali-Activated Binders. *J. Clean. Prod.* **2021**, *286*, 124972. [\[CrossRef\]](#)
- Elahi, M.M.A.; Hossain, M.M.; Karim, M.R.; Zain, M.F.M.; Shearer, C. A Review on Alkali-Activated Binders: Materials Composition and Fresh Properties of Concrete. *Constr. Build. Mater.* **2020**, *260*, 119788. [\[CrossRef\]](#)
- Çelikten, S.; Sandemir, M.; Deneme, İ.Ö. Mechanical and Microstructural Properties of Alkali-Activated Slag and Slag + fly Ash Mortars Exposed to High Temperature. *Constr. Build. Mater.* **2019**, *217*, 50–61. [\[CrossRef\]](#)
- Gijbels, K.; Iacobescu, R.I.; Pontikes, Y.; Schreurs, S.; Schroyers, W. Alkali-Activated Binders Based on Ground Granulated Blast Furnace Slag and Phosphogypsum. *Constr. Build. Mater.* **2019**, *215*, 371–380. [\[CrossRef\]](#)
- Wu, M.; Shen, W.; Xiong, X.; Zhao, L.; Yu, Z.; Sun, H.; Xu, G.; Zhao, Q.; Wang, G.; Zhang, W. Effects of the Phosphogypsum on the Hydration and Microstructure of Alkali Activated Slag Pastes. *Constr. Build. Mater.* **2023**, *368*, 130391. [\[CrossRef\]](#)
- Kim, T. Characteristics of Alkali-Activated Slag Cement-Based Ultra-Lightweight Concrete with High-Volume Cenosphere. *Constr. Build. Mater.* **2021**, *302*, 124165. [\[CrossRef\]](#)
- Zheng, Y.; Xuan, D.; Shen, B.; Ma, K. Shrinkage Mitigation of Alkali-Activated Fly Ash/Slag Mortar by Using Phosphogypsum Waste. *Constr. Build. Mater.* **2023**, *375*, 130978. [\[CrossRef\]](#)
- Pan, Z.; Tao, Z.; Cao, Y.F.; Wuhner, R.; Murphy, T. Compressive Strength and Microstructure of Alkali-Activated Fly Ash/Slag Binders at High Temperature. *Cem. Concr. Compos.* **2018**, *86*, 9–18. [\[CrossRef\]](#)
- Colangelo, F.; Cioffi, R.; Roviello, G.; Capasso, I.; Caputo, D.; Aprea, P.; Liguori, B.; Ferone, C. Thermal Cycling Stability of Fly Ash Based Geopolymer Mortars. *Compos. B Eng.* **2017**, *129*, 11–17. [\[CrossRef\]](#)

24. Huseien, G.F.; Sam, A.R.M.; Shah, K.W.; Mirza, J.; Tahir, M.M. Evaluation of Alkali-Activated Mortars Containing High Volume Waste Ceramic Powder and Fly Ash Replacing GBFS. *Constr. Build. Mater.* **2019**, *210*, 78–92. [[CrossRef](#)]
25. Olatoyan, O.J.; Kareem, M.A.; Adebajo, A.U.; Olawale, S.O.A.; Alao, K.T. Potential Use of Biomass Ash as a Sustainable Alternative for Fly Ash in Concrete Production: A Review. *Hybrid Adv.* **2023**, *4*, 100076. [[CrossRef](#)]
26. Ilari, A.; Duca, D.; Boakye-Yiadom, K.A.; Gasperini, T.; Toscano, G. Carbon Footprint and Feedstock Quality of a Real Biomass Power Plant Fed with Forestry and Agricultural Residues. *Resources* **2022**, *11*, 7. [[CrossRef](#)]
27. Silvestro, L.; Scolaro, T.P.; Ruviano, A.S.; Lima, G.T.d.S.; Gleize, P.J.P.; Pelisser, F. Use of Biomass Wood Ash to Produce Sustainable Geopolymeric Pastes. *Constr. Build. Mater.* **2023**, *370*, 130641. [[CrossRef](#)]
28. Pels, J.R.; Nie, D.S. De Utilization of Ashes from Biomass Combustion and Gasification. In Proceedings of the 14th European Biomass Conference & Exhibition, Paris, France, 17–21 October 2005.
29. Van Eijk, R.J. Options for Increased Utilization of Ash from Biomass Combustion and Co-Firing. In *IEA Bioenergy Task 32*; Kema: Arnhem, The Netherlands, 2012.
30. Santhosh, K.G.; Subhani, S.M.; Bahurudeen, A. Sustainable Reuse of Palm Oil Fuel Ash in Concrete, Alkali-Activated Binders, Soil Stabilisation, Bricks and Adsorbent: A Waste to Wealth Approach. *Ind. Crop. Prod.* **2022**, *183*, 114954. [[CrossRef](#)]
31. Santhosh, K.G.; Subhani, S.M.; Bahurudeen, A. Recycling of Palm Oil Fuel Ash and Rice Husk Ash in the Cleaner Production of Concrete. *J. Clean. Prod.* **2022**, *354*, 131736. [[CrossRef](#)]
32. Murugesan, T.; Vidjeapriya, R.; Bahurudeen, A. Development of Sustainable Alkali Activated Binder for Construction Using Sugarcane Bagasse Ash and Marble Waste. *Sugar Tech* **2020**, *22*, 885–895. [[CrossRef](#)]
33. Gedela Santhosh, K.; Subhani, S.M.; Bahurudeen, A. An Investigation on the Effectiveness of Quarry Dust and Sugarcane Bagasse Ash in Na-Based Alkali-Activated Binder. *Mater. Today Proc.* **2023**, *in press*. [[CrossRef](#)]
34. Chougan, M.; Ghaffar, S.H.; Sikora, P.; Mijowska, E.; Kukułka, W.; Stephan, D. Boosting Portland Cement-Free Composite Performance via Alkali-Activation and Reinforcement with Pre-Treated Functionalised Wheat Straw. *Ind. Crop. Prod.* **2022**, *178*, 114648. [[CrossRef](#)]
35. Das, D.; Laskar, S.M.; Hussain, B. Study on Slag-Rice Husk Ash Based Alkali Activated Concrete. *ASPS Conf. Proc.* **2022**, *1*, 147–151. [[CrossRef](#)]
36. Dhasindrakrishna, K.; Ramakrishnan, S.; Pasupathy, K.; Sanjayan, J. Synthesis and Performance of Intumescent Alkali-Activated Rice Husk Ash for Fire-Resistant Applications. *J. Build. Eng.* **2022**, *51*, 104281. [[CrossRef](#)]
37. Matalkah, F.; Soroushian, P.; Abideen, S.U.; Peyvandi, A. Use of Non-Wood Biomass Combustion Ash in Development of Alkali-Activated Concrete. *Constr. Build. Mater.* **2016**, *121*, 491–500. [[CrossRef](#)]
38. Zhu, C.J.; Pundienė, I.; Pranckevičienė, J.; Kligys, M.; Korjaks, A.; Vitola, L. Influence of Alkaline Activator Solution Ratio on the Properties of Biomass Fly Ash-Based Alkali-Activated Materials. *J. Phys. Conf. Ser.* **2023**, *2423*, 012033. [[CrossRef](#)]
39. Athira, V.S.; Charitha, V.; Athira, G.; Bahurudeen, A. Agro-Waste Ash Based Alkali-Activated Binder: Cleaner Production of Zero Cement Concrete for Construction. *J. Clean. Prod.* **2021**, *286*, 125429. [[CrossRef](#)]
40. Prabagar, S.; Thuraisingam, S.; Prabagar, J. The Influence of Eco-Friendly Ash on Sustainable Construction Material: A Review. *Appl. Sci. Innov. Res.* **2022**, *6*, 39. [[CrossRef](#)]
41. Das, S.K.; Adediran, A.; Kaze, C.R.; Mustakim, S.M.; Leklou, N. Production, Characteristics, and Utilization of Rice Husk Ash in Alkali Activated Materials: An Overview of Fresh and Hardened State Properties. *Constr. Build. Mater.* **2022**, *345*, 128341.
42. Ercan, E.E.T.; Andreas, L.; Cwirzen, A.; Habermehl-Cwirzen, K. Wood Ash as Sustainable Alternative Raw Material for the Production of Concrete—A Review. *Materials* **2023**, *16*, 2557. [[CrossRef](#)]
43. Wang, R.; Haller, P. Applications of Wood Ash as a Construction Material in Civil Engineering: A Review. *Biomass Conv. Biorefin.* **2022**, *1–21*. [[CrossRef](#)]
44. Martínez-García, R.; Jagadesh, P.; Zaid, O.; Şerbănoiu, A.A.; Fraile-Fernández, F.J.; de Prado-Gil, J.; Qaidi, S.M.A.; Grădinaru, C.M. The Present State of the Use of Waste Wood Ash as an Eco-Efficient Construction Material: A Review. *Materials* **2022**, *15*, 5349. [[CrossRef](#)] [[PubMed](#)]
45. Isa, M.N.; Awang, H.; Muthusamy, K. A Potential Environmental Sustainability of Wood Ash in Normal and Geopolymer Concrete—A Review. *Adv. Sci. Technol. Res. J.* **2023**, *17*, 1–20. [[CrossRef](#)] [[PubMed](#)]
46. Cabrera, M.; DíazLópez, J.L.; Agrela, F.; Rosales, J. Eco-efficient Cement-based Materials Using Biomass Bottom Ash: A Review. *Appl. Sci.* **2020**, *10*, 8026. [[CrossRef](#)]
47. AL-Kharabsheh, B.N.; Arbili, M.M.; Majdi, A.; Ahmad, J.; Deifalla, A.F.; Hakamy, A. A Review on Strength and Durability Properties of Wooden Ash Based Concrete. *Materials* **2022**, *15*, 7282. [[CrossRef](#)] [[PubMed](#)]
48. Ayobami, A.B. Performance of Wood Bottom Ash in Cement-Based Applications and Comparison with Other Selected Ashes: Overview. *Resour. Conserv. Recycl.* **2021**, *166*, 105351. [[CrossRef](#)]
49. Nascimento, L.C.; Junior, G.B.; Xavier, G.d.C.; Monteiro, S.N.; Vieira, C.M.F.; de Azevedo, A.R.G.; Alexandre, J. Use of Wood Bottom Ash in Cementitious Materials: A Review. *J. Mater. Res. Technol.* **2023**, *23*, 4226–4243. [[CrossRef](#)]
50. Tamanna, K.; Raman, S.N.; Jamil, M.; Hamid, R. Utilization of Wood Waste Ash in Construction Technology: A Review. *Constr. Build. Mater.* **2020**, *237*, 117654. [[CrossRef](#)]
51. Cheah, C.B.; Ramli, M. The Implementation of Wood Waste Ash as a Partial Cement Replacement Material in the Production of Structural Grade Concrete and Mortar: An Overview. *Resour. Conserv. Recycl.* **2011**, *55*, 669–685. [[CrossRef](#)]

52. Rajamma, R.; Senff, L.; Ribeiro, M.J.; Labrincha, J.A.; Ball, R.J.; Allen, G.C.; Ferreira, V.M. Biomass Fly Ash Effect on Fresh and Hardened State Properties of Cement Based Materials. *Compos. B Eng.* **2015**, *77*, 1–9. [[CrossRef](#)]
53. Berra, M.; Mangialardi, T.; Paolini, A.E. Reuse of Woody Biomass Fly Ash in Cement-Based Materials. *Constr. Build. Mater.* **2015**, *76*, 286–296. [[CrossRef](#)]
54. Barbosa, R.; Lapa, N.; Dias, D.; Mendes, B. Concretes Containing Biomass Ashes: Mechanical, Chemical, and Ecotoxic Performances. *Constr. Build. Mater.* **2013**, *48*, 457–463. [[CrossRef](#)]
55. Rissanen, J.; Ohenoja, K.; Kinnunen, P.; Romagnoli, M.; Illikainen, M. Milling of Peat-Wood Fly Ash: Effect on Water Demand of Mortar and Rheology of Cement Paste. *Constr. Build. Mater.* **2018**, *180*, 143–153. [[CrossRef](#)]
56. Nagrockienė, D.; Daugėla, A. Investigation into the Properties of Concrete Modified with Biomass Combustion Fly Ash. *Constr. Build. Mater.* **2018**, *174*, 369–375. [[CrossRef](#)]
57. Vassilev, S.V.; Baxter, D.; Andersen, L.K.; Vassileva, C.G. An Overview of the Composition and Application of Biomass Ash. Part 1. Phase-Mineral and Chemical Composition and Classification. *Fuel* **2013**, *105*, 40–76. [[CrossRef](#)]
58. Gómez-Casero, M.A.; Pérez-Villarejo, L.; Castro, E.; Eliche-Quesada, D. Effect of Steel Slag and Curing Temperature on the Improvement in Technological Properties of Biomass Bottom Ash Based Alkali-Activated Materials. *Constr. Build. Mater.* **2021**, *302*, 124205. [[CrossRef](#)]
59. Maschowski, C.; Kruspan, P.; Garra, P.; Arif, A.T.; Trouvé, G.; Gieré, R. Physicochemical and Mineralogical Characterization of Biomass Ash from Different Power Plants in the Upper Rhine Region. *Fuel* **2019**, *258*, 116020. [[CrossRef](#)] [[PubMed](#)]
60. Sathonsaowaphak, A.; Chindaprasirt, P.; Pimraksa, K. Workability and Strength of Lignite Bottom Ash Geopolymer Mortar. *J. Hazard. Mater.* **2009**, *168*, 44–50. [[CrossRef](#)]
61. Zhu, C.; Pundienė, I.; Pranckevičienė, J.; Kligys, M. Effects of Na<sub>2</sub>CO<sub>3</sub>/Na<sub>2</sub>SiO<sub>3</sub> Ratio and Curing Temperature on the Structure Formation of Alkali-Activated High-Carbon Biomass Fly Ash Pastes. *Materials* **2022**, *15*, 8354. [[CrossRef](#)]
62. Fernández-Jiménez, A.; Palomo, A. Characterisation of Fly Ashes. Potential Reactivity as Alkaline Cements. *Fuel* **2003**, *82*, 2259–2265. [[CrossRef](#)]
63. Antunes Boca Santa, R.A.; Soares, C.; Riella, H.G. Geopolymers Obtained from Bottom Ash as Source of Aluminosilicate Cured at Room Temperature. *Constr. Build. Mater.* **2017**, *157*, 459–466. [[CrossRef](#)]
64. Saeli, M.; Senff, L.; Tobaldi, D.M.; Seabra, M.P.; Labrincha, J.A. Novel Biomass Fly Ash-Based Geopolymeric Mortars Using Lime Slaker Grits as Aggregate for Applications in Construction: Influence of Granulometry and Binder/Aggregate Ratio. *Constr. Build. Mater.* **2019**, *227*, 116643. [[CrossRef](#)]
65. Silva, T.H.; Lara, L.F.S.; Silva, G.J.B.; Provis, J.L.; Bezerra, A.C.S. Alkali-Activated Materials Produced Using High-Calcium, High-Carbon Biomass Ash. *Cem. Concr. Compos.* **2022**, *132*, 104646. [[CrossRef](#)]
66. Carević, I.; Baričević, A.; Štirmer, N.; Šantek Bajto, J. Correlation between Physical and Chemical Properties of Wood Biomass Ash and Cement Composites Performances. *Constr. Build. Mater.* **2020**, *256*, 119450. [[CrossRef](#)]
67. Rajamma, R.; Ball, R.J.; Tarelho, L.A.C.; Allen, G.C.; Labrincha, J.A.; Ferreira, V.M. Characterisation and Use of Biomass Fly Ash in Cement-Based Materials. *J. Hazard. Mater.* **2009**, *172*, 1049–1060. [[CrossRef](#)]
68. Ngueyep, M.; Leroy, L. Valorization of Wood Ashes as Partial Replacement of Portland Cement: Mechanical Performance and Durability. *Eur. J. Sci. Res.* **2019**, *151*, 468–478.
69. Carević, I.; Serdar, M.; Štirmer, N.; Ukrainczyk, N. Preliminary Screening of Wood Biomass Ashes for Partial Resources Replacements in Cementitious Materials. *J. Clean. Prod.* **2019**, *229*, 1045–1064. [[CrossRef](#)]
70. Thi, K.D.T.; Liao, M.C.; Vo, D.H. The Characteristics of Alkali-Activated Slag-Fly Ash Incorporating the High Volume Wood Bottom Ash: Mechanical Properties and Microstructures. *Constr. Build. Mater.* **2023**, *394*, 132240. [[CrossRef](#)]
71. Ates, F.; Park, K.T.; Kim, K.W.; Woo, B.H.; Kim, H.G. Effects of Treated Biomass Wood Fly Ash as a Partial Substitute for Fly Ash in a Geopolymer Mortar System. *Constr. Build. Mater.* **2023**, *376*, 131063. [[CrossRef](#)]
72. Vaičiukynienė, D.; Nizevičienė, D.; Kantautas, A.; Bocullo, V.; Kiele, A. Alkali Activated Paste and Concrete Based on of Biomass Bottom Ash with Phosphogypsum. *Appl. Sci.* **2020**, *10*, 5190. [[CrossRef](#)]
73. Vaičiukynienė, D.; Nizevičienė, D.; Mikelionienė, A.; Radzevičius, A. Utilization of Zeolitic Waste in Alkali-Activated Biomass Bottom Ash Blends. *Molecules* **2020**, *25*, 3053. [[CrossRef](#)]
74. Vaičiukynienė, D.; Nizevičienė, D.; Kantautas, A.; Kielė, A.; Bocullo, V. Alkali Activated Binders Based on Biomass Bottom Ash and Silica By-Product Blends. *Waste Biomass Valorization* **2021**, *12*, 1095–1105. [[CrossRef](#)]
75. Silva, G.J.B.; Santana, V.P.; Wójcik, M. Investigation on Mechanical and Microstructural Properties of Alkali-Activated Materials Made of Wood Biomass Ash and Glass Powder. *Powder Technol.* **2021**, *377*, 900–912. [[CrossRef](#)]
76. Lin, J.; Tan, T.H.; Yeo, J.S.; Goh, Y.; Ling, T.C.; Mo, K.H. Municipal Woody Biomass Waste Ash-Based Cold-Bonded Artificial Lightweight Aggregate Produced by One-Part Alkali-Activation Method. *Constr. Build. Mater.* **2023**, *394*, 131619. [[CrossRef](#)]
77. Abdulkareem, O.A.; Ramli, M.; Matthews, J.C. Production of Geopolymer Mortar System Containing High Calcium Biomass Wood Ash as a Partial Substitution to Fly Ash: An Early Age Evaluation. *Compos. B Eng.* **2019**, *174*, 106941. [[CrossRef](#)]
78. Hassan, H.S.; Abdel-Gawwad, H.A.; Vásquez-García, S.R.; Israde-Alcántara, I.; Flores-Ramirez, N.; Rico, J.L.; Mohammed, M.S. Cleaner Production of One-Part White Geopolymer Cement Using Pre-Treated Wood Biomass Ash and Diatomite. *J. Clean. Prod.* **2019**, *209*, 1420–1428. [[CrossRef](#)]
79. De Rossi, A.; Simão, L.; Ribeiro, M.J.; Hotza, D.; Moreira, R.F.P.M. Study of Cure Conditions Effect on the Properties of Wood Biomass Fly Ash Geopolymers. *J. Mater. Res. Technol.* **2020**, *9*, 7518–7528. [[CrossRef](#)]

80. Eliche-Quesada, D.; Calero-Rodríguez, A.; Bonet-Martínez, E.; Pérez-Villarejo, L.; Sánchez-Soto, P.J. Geopolymers Made from Metakaolin Sources, Partially Replaced by Spanish Clays and Biomass Bottom Ash. *J. Build. Eng.* **2021**, *40*, 102761. [[CrossRef](#)]
81. Jurado-Contreras, S.; Bonet-Martínez, E.; Sánchez-Soto, P.J.; Gencel, O.; Eliche-Quesada, D. Synthesis and Characterization of Alkali-Activated Materials Containing Biomass Fly Ash and Metakaolin: Effect of the Soluble Salt Content of the Residue. *Arch. Civ. Mech. Eng.* **2022**, *22*, 121. [[CrossRef](#)]
82. Bijeljić, J.; Ristić, N.; Grdić, D.; Pavlović, M. Possibilities of Biomass Wood Ash Usage in Geopolymer Mixtures. *Teh. Vjesn.* **2023**, *30*, 52–60. [[CrossRef](#)]
83. Sitarz-Palczak, E.; Kalembkiewicz, J.; Galas, D. Comparative Study on the Characteristics of Coal Fly Ash and Biomass Ash Geopolymers. *Arch. Environ. Prot.* **2019**, *45*, 126–135. [[CrossRef](#)]
84. De, S.; Mishra, S.; Poonguzhali, E.; Rajesh, M.; Tamilarasan, K. Fractionation and Characterization of Lignin from Waste Rice Straw: Biomass Surface Chemical Composition Analysis. *Int. J. Biol. Macromol.* **2020**, *145*, 795–803. [[CrossRef](#)] [[PubMed](#)]
85. Etiégni, L.; Campbell, A.G. Physical and Chemical Characteristics of Wood Ash. *Bioresour. Technol.* **1991**, *37*, 173–178. [[CrossRef](#)]
86. Karrech, A.; Dong, M.; Elchalakani, M.; Shahin, M.A. Sustainable Geopolymer Using Lithium Concentrate Residues. *Constr. Build. Mater.* **2019**, *228*, 116740. [[CrossRef](#)]
87. Shi, C.; Krivenko, P.V.; Roy, D. *Alkali-Activated Cements and Concretes*; CRC Press: London, UK, 2006.
88. Li, C.; Sun, H.; Li, L. A Review: The Comparison between Alkali-Activated Slag (Si + Ca) and Metakaolin (Si + Al) Cements. *Cem. Concr. Res.* **2010**, *40*, 1341–1349. [[CrossRef](#)]
89. Mohammed, B.S.; Haruna, S.; Wahab, M.M.A.; Liew, M.S.; Haruna, A. Mechanical and Microstructural Properties of High Calcium Fly Ash One-Part Geopolymer Cement Made with Granular Activator. *Heliyon* **2019**, *5*, e022552019. [[CrossRef](#)]
90. Lee, W.K.W.; Van Deventer, J.S.J. The Effect of Ionic Contaminants on the Early-Age Properties of Alkali-Activated Fly Ash-Based Cements. *Cem. Concr. Res.* **2002**, *32*, 577–584. [[CrossRef](#)]
91. Puligilla, S.; Mondal, P. Role of Slag in Microstructural Development and Hardening of Fly Ash-Slag Geopolymer. *Cem. Concr. Res.* **2013**, *43*, 70–80. [[CrossRef](#)]
92. Kim, E.H. Understanding Effects of Silicon/Aluminum Ratio and Calcium Hydroxide on Chemical Composition, Nanostructure and Compressive Strength for Metakaolin Geopolymers. Master's Thesis, University of Illinois at Urbana-Champaign, Urbana, IL, USA, 2012.
93. de la Grée, G.C.H.D.; Florea, M.V.A.; Keulen, A.; Brouwers, H.J.H. Contaminated Biomass Fly Ashes—Characterization and Treatment Optimization for Reuse as Building Materials. *Waste Manag.* **2016**, *49*, 96–109. [[CrossRef](#)]
94. Peng, Y.-X.; Ni, X.; Zhu, Z.-C.; Yu, Z.-F.; Yin, Z.-X.; Li, T.-Q.; Liu, S.-Y.; Zhao, L.-L.; Xu, J. Friction and Wear of Liner and Grinding Ball in Iron Ore Ball Mill. *Tribol. Int.* **2017**, *115*, 506–517. [[CrossRef](#)]
95. Kumar, S.; Kumar, R. Mechanical Activation of Fly Ash: Effect on Reaction, Structure and Properties of Resulting Geopolymer. *Ceram. Int.* **2011**, *37*, 533–541. [[CrossRef](#)]
96. Hamzaoui, R.; Bouchenafa, O.; Guessasma, S.; Leklou, N.; Bouaziz, A. The Sequel of Modified Fly Ashes Using High Energy Ball Milling on Mechanical Performance of Substituted Past Cement. *Mater. Des.* **2016**, *90*, 29–37. [[CrossRef](#)]
97. Amaral, R.C.; Rohden, A.B.; Garcez, M.R.; Andrade, J.J.d.O. Reuse of Wood Ash from Biomass Combustion in Non-Structural Concrete: Mechanical Properties, Durability, and Eco-Efficiency. *J. Mater. Cycles Waste Manag.* **2022**, *24*, 2439–2454. [[CrossRef](#)]
98. Komljenović, M.; Bašcarević, Z.; Bradić, V. Mechanical and Microstructural Properties of Alkali-Activated Fly Ash Geopolymers. *J. Hazard. Mater.* **2010**, *181*, 35–42. [[CrossRef](#)] [[PubMed](#)]
99. Tchakouté, H.K.; Rüscher, C.H.; Kong, S.; Kamsu, E.; Leonelli, C. Geopolymer Binders from Metakaolin Using Sodium Waterglass from Waste Glass and Rice Husk Ash as Alternative Activators: A Comparative Study. *Constr. Build. Mater.* **2016**, *114*, 276–289. [[CrossRef](#)]
100. Turner, L.K.; Collins, F.G. Carbon Dioxide Equivalent (CO<sub>2</sub>-e) Emissions: A Comparison between Geopolymer and OPC Cement Concrete. *Constr. Build. Mater.* **2013**, *43*, 125–130. [[CrossRef](#)]
101. Jeon, D.; Jun, Y.; Jeong, Y.; Oh, J.E. Microstructural and Strength Improvements through the Use of Na<sub>2</sub>CO<sub>3</sub> in a Cementless Ca(OH)<sub>2</sub>-Activated Class F Fly Ash System. *Cem. Concr. Res.* **2015**, *67*, 215–225. [[CrossRef](#)]
102. Khale, D.; Chaudhary, R. Mechanism of Geopolymerization and Factors Influencing Its Development: A Review. *J. Mater. Sci.* **2007**, *42*, 729–746. [[CrossRef](#)]
103. Phair, J.W.; Van Deventer, J.S.J. Effect of Silicate Activator PH on the Leaching and Material Characteristics of Waste-Based Inorganic Polymers. *Miner. Eng.* **2001**, *14*, 289–304. [[CrossRef](#)]
104. Xu, H.; Van Deventer, J.S.J. The Geopolymerisation of Alumino-Silicate Minerals. *Int. J. Miner. Process.* **2000**, *59*, 247–266. [[CrossRef](#)]
105. PQ Europe Sodium and Potassium Silicates. Sodium and Potassium Silicates: Versatile Compounds for Your Applications. 2004, 2. Available online: <https://www.scribd.com/document/382255676/sodium-and-potassium-silicates-brochure-eng-oct-2004-pdf> (accessed on 1 April 2024).
106. Singh, B.; Rahman, M.R.; Paswan, R.; Bhattacharyya, S.K. Effect of Activator Concentration on the Strength, ITZ and Drying Shrinkage of Fly Ash/Slag Geopolymer Concrete. *Constr. Build. Mater.* **2016**, *118*, 171–179. [[CrossRef](#)]
107. Ishwarya, G.; Singh, B.; Deshwal, S.; Bhattacharyya, S.K. Effect of Sodium Carbonate/Sodium Silicate Activator on the Rheology, Geopolymerization and Strength of Fly Ash/Slag Geopolymer Pastes. *Cem. Concr. Compos.* **2019**, *97*, 226–238. [[CrossRef](#)]

108. Chithiraputhiran, S.; Neithalath, N. Isothermal Reaction Kinetics and Temperature Dependence of Alkali Activation of Slag, Fly Ash and Their Blends. *Constr. Build. Mater.* **2013**, *45*, 233–242. [[CrossRef](#)]
109. Xu, H.; Gong, W.; Syltebo, L.; Izzo, K.; Lutze, W.; Pegg, I.L. Effect of Blast Furnace Slag Grades on Fly Ash Based Geopolymer Waste Forms. *Fuel* **2014**, *133*, 332–340. [[CrossRef](#)]
110. Rajamma, R.; Labrincha, J.A.; Ferreira, V.M. Alkali Activation of Biomass Fly Ash-Metakaolin Blends. *Fuel* **2012**, *98*, 265–271. [[CrossRef](#)]
111. Rodrigue Kaze, C.; Ninla Lemougna, P.; Alomayri, T.; Assaedi, H.; Adesina, A.; Kumar Das, S.; Lecomte-Nana, G.L.; Kamseu, E.; Chinje Melo, U.; Leonelli, C. Characterization and Performance Evaluation of Laterite Based Geopolymer Binder Cured at Different Temperatures. *Constr. Build. Mater.* **2021**, *270*, 121443. [[CrossRef](#)]
112. Zribi, M.; Samet, B.; Baklouti, S. Effect of Curing Temperature on the Synthesis, Structure and Mechanical Properties of Phosphate-Based Geopolymers. *J. Non Cryst. Solids* **2019**, *511*, 62–67. [[CrossRef](#)]
113. Mustafa Al Bakri, A.M.; Kamarudin, H.; Bnhussain, M.; Nizar, K.; Rafiza, A.R.; Zarina, Y. The Processing, Characterization, and Properties of Fly Ash Based Geopolymer Concrete. *Rev. Adv. Mater. Sci.* **2012**, *30*, 90–97.
114. Ozer, I.; Soyer-Uzun, S. Relations between the Structural Characteristics and Compressive Strength in Metakaolin Based Geopolymers with Different Molar Si/Al Ratios. *Ceram. Int.* **2015**, *41*, 10192–10198. [[CrossRef](#)]
115. Zhang, Z.; Wang, H.; Reid, A.; Aravinthan, T. Effects of Fly Ash Source and Curing Procedure on Strength Development of Geopolymers. In Proceedings of the Incorporating Sustainable Practice in Mechanics of Structures and Materials—Proceedings of the 21st Australian Conference on the Mechanics of Structures and Materials, Melbourne, Australia, 7–10 December 2010; Scimago Journal & Country Rank: Granada, Spain, 2011.
116. Cheah, C.B.; Part, W.K.; Ramli, M. The Hybridizations of Coal Fly Ash and Wood Ash for the Fabrication of Low Alkalinity Geopolymer Load Bearing Block Cured at Ambient Temperature. *Constr. Build. Mater.* **2015**, *88*, 41–55. [[CrossRef](#)]
117. Sun, B.; Sun, Y.; Ye, G.; De Schutter, G. A Mix Design Methodology of Slag and Fly Ash-Based Alkali-Activated Paste. *Cem. Concr. Compos.* **2022**, *126*, 104368. [[CrossRef](#)]
118. Bernal, S.A.; Provis, J.L.; Myers, R.J.; San Nicolas, R.; van Deventer, J.S.J. Role of Carbonates in the Chemical Evolution of Sodium Carbonate-Activated Slag Binders. *Mater. Struct.* **2014**, *48*, 517–529. [[CrossRef](#)]
119. Cheah, C.B.; Ramli, M. The Engineering Properties of High Performance Concrete with HCWA-DSF Supplementary Binder. *Constr. Build. Mater.* **2013**, *40*, 93–103. [[CrossRef](#)]
120. Yip, C.K.; Lukey, G.C.; Van Deventer, J.S.J. The Coexistence of Geopolymeric Gel and Calcium Silicate Hydrate at the Early Stage of Alkaline Activation. *Cem. Concr. Res.* **2005**, *35*, 1688–1697. [[CrossRef](#)]
121. Gallé, C. Effect of Drying on Cement-Based Materials Pore Structure as Identified by Mercury Intrusion Porosimetry—A Comparative Study between Oven-, Vacuum-, and Freeze-Drying. *Cem. Concr. Res.* **2001**, *31*, 1467–1477. [[CrossRef](#)]
122. Nemaleu, J.G.D.; Kaze, R.C.; Tome, S.; Alomayri, T.; Assaedi, H.; Kamseu, E.; Melo, U.C.; Sglavo, V.M. Powdered Banana Peel in Calcined Halloysite Replacement on the Setting Times and Engineering Properties on the Geopolymer Binders. *Constr. Build. Mater.* **2021**, *279*, 122480. [[CrossRef](#)]
123. Rovnaník, P. Effect of Curing Temperature on the Development of Hard Structure of Metakaolin-Based Geopolymer. *Constr. Build. Mater.* **2010**, *24*, 1176–1183. [[CrossRef](#)]
124. Fernández-Jiménez, A.; Palomo, A. Composition and Microstructure of Alkali Activated Fly Ash Binder: Effect of the Activator. *Cem. Concr. Res.* **2005**, *35*, 1984–1992. [[CrossRef](#)]
125. Košnář, Z.; Mercl, F.; Perná, I.; Tlustoš, P. Investigation of Polycyclic Aromatic Hydrocarbon Content in Fly Ash and Bottom Ash of Biomass Incineration Plants in Relation to the Operating Temperature and Unburned Carbon Content. *Sci. Total Environ.* **2016**, *563–564*, 53–61. [[CrossRef](#)]
126. Perná, I.; Šupová, M.; Hanzlíček, T.; Špaldonová, A. The Synthesis and Characterization of Geopolymers Based on Metakaolin and High LOI Straw Ash. *Constr. Build. Mater.* **2019**, *228*, 116765. [[CrossRef](#)]
127. Yuan, J.; He, P.; Jia, D.; Yang, C.; Zhang, Y.; Yan, S.; Yang, Z.; Duan, X.; Wang, S.; Zhou, Y. Effect of Curing Temperature and SiO<sub>2</sub>/K<sub>2</sub>O Molar Ratio on the Performance of Metakaolin-Based Geopolymers. *Ceram. Int.* **2016**, *42*, 16184–16190. [[CrossRef](#)]
128. Le, T.; Wang, Q.; Ravindra, A.V.; Li, X.; Ju, S. Microwave Intensified Synthesis of Zeolite-Y from Spent FCC Catalyst after Acid Activation. *J. Alloys Compd.* **2019**, *776*, 437–446. [[CrossRef](#)]
129. Huseien, G.F.; Ismail, M.; Khalid, N.H.A.; Hussin, M.W.; Mirza, J. Compressive Strength and Microstructure of Assorted Wastes Incorporated Geopolymer Mortars: Effect of Solution Molarity. *Alex. Eng. J.* **2018**, *57*, 3375–3386. [[CrossRef](#)]
130. Oh, J.E.; Monteiro, P.J.M.; Jun, S.S.; Choi, S.; Clark, S.M. The Evolution of Strength and Crystalline Phases for Alkali-Activated Ground Blast Furnace Slag and Fly Ash-Based Geopolymers. *Cem. Concr. Res.* **2010**, *40*, 189–196. [[CrossRef](#)]
131. Timakul, P.; Rattanaprasit, W.; Aungkavattana, P. Improving Compressive Strength of Fly Ash-Based Geopolymer Composites by Basalt Fibers Addition. *Ceram. Int.* **2016**, *42*, 6288–6295. [[CrossRef](#)]
132. Fernández-Jiménez, A.; Cristelo, N.; Miranda, T.; Palomo, Á. Sustainable Alkali Activated Materials: Precursor and Activator Derived from Industrial Wastes. *J. Clean. Prod.* **2017**, *162*, 1200–1209. [[CrossRef](#)]
133. Zhang, M.; Guo, H.; El-Korchi, T.; Zhang, G.; Tao, M. Experimental Feasibility Study of Geopolymer as the Next-Generation Soil Stabilizer. *Constr. Build. Mater.* **2013**, *47*, 1468–1478. [[CrossRef](#)]
134. Sore, S.O.; Messan, A.; Prud'homme, E.; Escadeillas, G.; Tsobnang, F. Synthesis and Characterization of Geopolymer Binders Based on Local Materials from Burkina Faso—Metakaolin and Rice Husk Ash. *Constr. Build. Mater.* **2016**, *124*, 301–311. [[CrossRef](#)]

135. De Rossi, A.; Simão, L.; Ribeiro, M.J.; Novais, R.M.; Labrincha, J.A.; Hotza, D.; Moreira, R.F.P.M. In-Situ Synthesis of Zeolites by Geopolymerization of Biomass Fly Ash and Metakaolin. *Mater. Lett.* **2019**, *236*, 644–648. [[CrossRef](#)]
136. de Moraes Pinheiro, S.M.; Font, A.; Soriano, L.; Tashima, M.M.; Monzó, J.; Borrachero, M.V.; Payá, J. Olive-Stone Biomass Ash (OBA): An Alternative Alkaline Source for the Blast Furnace Slag Activation. *Constr. Build. Mater.* **2018**, *178*, 327–338. [[CrossRef](#)]
137. Firdous, R.; Hirsch, T.; Klimm, D.; Lothenbach, B.; Stephan, D. Reaction of Calcium Carbonate Minerals in Sodium Silicate Solution and Its Role in Alkali-Activated Systems. *Miner. Eng.* **2021**, *165*, 106849. [[CrossRef](#)]
138. Sun, R.; Fang, C.; Zhang, H.; Ling, Y.; Feng, J.; Qi, H.; Ge, Z. Chemo-Mechanical Properties of Alkali-Activated Slag/Fly Ash Paste Incorporating White Mud. *Constr. Build. Mater.* **2021**, *291*, 123312. [[CrossRef](#)]
139. Van Jaarsveld, J.G.S.; Van Deventer, J.S.J.; Lukey, G.C. The Effect of Composition and Temperature on the Properties of Fly Ash- and Kaolinite-Based Geopolymers. *Chem. Eng. J.* **2002**, *89*, 63–73. [[CrossRef](#)]
140. Le Troëdec, M.; Dalmay, P.; Patapy, C.; Peyratout, C.; Smith, A.; Chotard, T. Mechanical Properties of Hemp-Lime Reinforced Mortars: Influence of the Chemical Treatment of Fibers. *J. Compos. Mater.* **2011**, *45*, 2347–2357. [[CrossRef](#)]
141. Tchakoute, H.K.; Elimbi, A.; Yanne, E.; Djangang, C.N. Utilization of Volcanic Ashes for the Production of Geopolymers Cured at Ambient Temperature. *Cem. Concr. Compos.* **2013**, *38*, 75–81. [[CrossRef](#)]
142. Bayiha, B.N.; Billong, N.; Yamb, E.; Kaze, R.C.; Nzengwa, R. Effect of Limestone Dosages on Some Properties of Geopolymer from Thermally Activated Halloysite. *Constr. Build. Mater.* **2019**, *217*, 28–35. [[CrossRef](#)]
143. Nana, A.; Alomayri, T.S.; Venyite, P.; Kaze, R.C.; Assaedi, H.S.; Nobouassia, C.B.; Sontia, J.V.M.; Ngouné, J.; Kamseu, E.; Leonelli, C. Mechanical Properties and Microstructure of a Metakaolin-Based Inorganic Polymer Mortar Reinforced with Quartz Sand. *Silicon* **2022**, *14*, 263–274. [[CrossRef](#)]
144. Cheah, C.B.; Part, W.K.; Ramli, M. The Long Term Engineering Properties of Cementless Building Block Work Containing Large Volume of Wood Ash and Coal Fly Ash. *Constr. Build. Mater.* **2017**, *143*, 522–536. [[CrossRef](#)]
145. Mathivet, V.; Jouin, J.; Gharzouni, A.; Sobrados, I.; Celerier, H.; Rossignol, S.; Parlier, M. Acid-Based Geopolymers: Understanding of the Structural Evolutions during Consolidation and after Thermal Treatments. *J. Non Cryst. Solids* **2019**, *512*, 90–97. [[CrossRef](#)]
146. Ma, Y.; Ye, G.; Hu, J. Micro-Mechanical Properties of Alkali-Activated Fly Ash Evaluated by Nanoindentation. *Constr. Build. Mater.* **2017**, *147*, 407–416. [[CrossRef](#)]
147. Tchakouté, H.K.; Rüscher, C.H. Mechanical and Microstructural Properties of Metakaolin-Based Geopolymer Cements from Sodium Waterglass and Phosphoric Acid Solution as Hardeners: A Comparative Study. *Appl. Clay Sci.* **2017**, *140*, 81–87. [[CrossRef](#)]
148. Huo, Z.; Xu, X.; Lü, Z.; Song, J.; He, M.; Li, Z.; Wang, Q.; Yan, L. Synthesis of Zeolite NaP with Controllable Morphologies. *Microporous Mesoporous Mater.* **2012**, *158*, 137–140. [[CrossRef](#)]
149. Moudio, A.M.N.; Tchakouté, H.K.; Ngnintedem, D.L.V.; Andreola, F.; Kamseu, E.; Nanseu-Njiki, C.P.; Leonelli, C.; Rüscher, C.H. Influence of the Synthetic Calcium Aluminate Hydrate and the Mixture of Calcium Aluminate and Silicate Hydrates on the Compressive Strengths and the Microstructure of Metakaolin-Based Geopolymer Cements. *Mater. Chem. Phys.* **2021**, *264*, 124459. [[CrossRef](#)]
150. Hu, X.; Shi, C.; Shi, Z.; Zhang, L. Compressive Strength, Pore Structure and Chloride Transport Properties of Alkali-Activated Slag/Fly Ash Mortars. *Cem. Concr. Compos.* **2019**, *104*, 103392. [[CrossRef](#)]
151. Sun, B.; Ye, G.; de Schutter, G. A Review: Reaction Mechanism and Strength of Slag and Fly Ash-Based Alkali-Activated Materials. *Constr. Build. Mater.* **2022**, *326*, 126843. [[CrossRef](#)]
152. Gao, X.; Yu, Q.L.; Brouwers, H.J.H. Reaction Kinetics, Gel Character and Strength of Ambient Temperature Cured Alkali Activated Slag-Fly Ash Blends. *Constr. Build. Mater.* **2015**, *80*, 105–115. [[CrossRef](#)]
153. Cheah, C.B.; Samsudin, M.H.; Ramli, M.; Part, W.K.; Tan, L.E. The Use of High Calcium Wood Ash in the Preparation of Ground Granulated Blast Furnace Slag and Pulverized Fly Ash Geopolymers: A Complete Microstructural and Mechanical Characterization. *J. Clean. Prod.* **2017**, *156*, 114–123. [[CrossRef](#)]
154. Puertas, F.; González-Fonteboa, B.; González-Taboada, I.; Alonso, M.M.; Torres-Carrasco, M.; Rojo, G.; Martínez-Abella, F. Alkali-Activated Slag Concrete: Fresh and Hardened Behaviour. *Cem. Concr. Compos.* **2018**, *85*, 22–31. [[CrossRef](#)]
155. Fu, Q.; Bu, M.; Zhang, Z.; Xu, W.; Yuan, Q.; Niu, D. Hydration Characteristics and Microstructure of Alkali-Activated Slag Concrete: A Review. *Engineering* **2023**, *20*, 162–179. [[CrossRef](#)]
156. Caldas, L.R.; Saraiva, A.B.; Lucena, A.F.P.; Da Gloria, M.Y.; Santos, A.S.; Filho, R.D.T. Building Materials in a Circular Economy: The Case of Wood Waste as CO<sub>2</sub>-Sink in Bio Concrete. *Resour. Conserv. Recycl.* **2021**, *166*, 105346. [[CrossRef](#)]
157. Ohenoja, K.; Rissanen, J.; Kinnunen, P.; Illikainen, M. Direct Carbonation of Peat-Wood Fly Ash for Carbon Capture and Utilization in Construction Application. *J. CO<sub>2</sub> Util.* **2020**, *40*, 101203. [[CrossRef](#)]
158. Kannan, V.; Raja Priya, P. Evaluation of the Permeability of High Strength Concrete Using Metakaolin and Wood Ash as Partial Replacement for Cement. *SN Appl. Sci.* **2021**, *3*, 90. [[CrossRef](#)]
159. Gaudreault, C.; Lama, I.; Sain, D. Is the Beneficial Use of Wood Ash Environmentally Beneficial? A Screening-Level Life Cycle Assessment and Uncertainty Analysis. *J. Ind. Ecol.* **2020**, *24*, 1300–1309. [[CrossRef](#)]
160. Celik, K.; Meral, C.; Petek Gursel, A.; Mehta, P.K.; Horvath, A.; Monteiro, P.J.M. Mechanical Properties, Durability, and Life-Cycle Assessment of Self-Consolidating Concrete Mixtures Made with Blended Portland Cements Containing Fly Ash and Limestone Powder. *Cem. Concr. Compos.* **2015**, *56*, 59–72. [[CrossRef](#)]

161. Šķēls, P.; Bondars, K.; Plonis, R.; Haritonovs, V.; Paeglītis, A. Usage of Wood Fly Ash in Stabilization of Unbound Pavement Layers and Soils. In Proceedings of the 13th Baltic Sea Geotechnical Conference “Historical Experiences and Challenges of Geotechnical Problems in Baltic Sea Region”, Vilnius, Lithuania, 15–17 September 2016.
162. da Costa, T.P.; Quinteiro, P.; Arroja, L.; Dias, A.C. Environmental Performance of Different End-of-Life Alternatives of Wood Fly Ash by a Consequential Perspective. *Sustain. Mater. Technol.* **2022**, *32*, e004112022. [[CrossRef](#)]
163. da Costa, T.P.; Quinteiro, P.; Tarelho, L.A.C.; Arroja, L.; Dias, A.C. Environmental Assessment of Valorisation Alternatives for Woody Biomass Ash in Construction Materials. *Resour. Conserv. Recycl.* **2019**, *148*, 67–79. [[CrossRef](#)]
164. Amiandamhen, S.O.; Adamopoulos, S.; Adl-Zarrabi, B.; Yin, H.; Norén, J. Recycling Sawmilling Wood Chips, Biomass Combustion Residues, and Tyre Fibres into Cement-Bonded Composites: Properties of Composites and Life Cycle Analysis. *Constr. Build. Mater.* **2021**, *297*, 123781. [[CrossRef](#)]
165. Gabrijel, I.; Rukavina, M.J.; Štirmer, N. Influence of Wood Fly Ash on Concrete Properties through Filling Effect Mechanism. *Materials* **2021**, *14*, 7164. [[CrossRef](#)]
166. Kim, K.W.; Park, K.T.; Ates, F.; Kim, H.G.; Woo, B.H. Effect of Pretreated Biomass Fly Ash on the Mechanical Properties and Durability of Cement Mortar. *Case Stud. Constr. Mater.* **2023**, *18*, e017542023. [[CrossRef](#)]
167. Vilutiene, T.; Kalibatiene, D.; Hosseini, M.R.; Pellicer, E.; Zavadskas, E.K. Building Information Modeling (BIM) for Structural Engineering: A Bibliometric Analysis of the Literature. *Adv. Civ. Eng.* **2019**, *2019*, 5290690. [[CrossRef](#)]
168. Waltman, L.; Van Eck, N.J. A Smart Local Moving Algorithm for Large-Scale Modularity-Based Community Detection. *Eur. Phys. J. B* **2013**, *86*, 471. [[CrossRef](#)]
169. Hosseini, M.R.; Maghrebi, M.; Akbarnezhad, A.; Martek, I.; Arashpour, M. Analysis of Citation Networks in Building Information Modeling Research. *J. Constr. Eng. Manag.* **2018**, *144*, 04018064. [[CrossRef](#)]
170. Turk, J.; Cotič, Z.; Mladenovič, A.; Šajna, A. Environmental Evaluation of Green Concretes versus Conventional Concrete by Means of LCA. *Waste Manag.* **2015**, *45*, 194–205. [[CrossRef](#)] [[PubMed](#)]
171. Ghufuran, M.; Khan, K.I.A.; Ullah, F.; Nasir, A.R.; Al Alahmadi, A.A.; Alzaed, A.N.; Alwetaishi, M. Circular Economy in the Construction Industry: A Step towards Sustainable Development. *Buildings* **2022**, *12*, 1004. [[CrossRef](#)]
172. Norouzi, M.; Chàfer, M.; Cabeza, L.F.; Jiménez, L.; Boer, D. Circular Economy in the Building and Construction Sector: A Scientific Evolution Analysis. *J. Build. Eng.* **2021**, *44*, 102704. [[CrossRef](#)]
173. Usta, M.C.; Yörük, C.R.; Uibu, M.; Hain, T.; Gregor, A.; Trikkel, A. CO<sub>2</sub> Curing of Ca-Rich Fly Ashes to Produce Cement-Free Building Materials. *Minerals* **2022**, *12*, 513. [[CrossRef](#)]

**Disclaimer/Publisher’s Note:** The statements, opinions and data contained in all publications are solely those of the individual author(s) and contributor(s) and not of MDPI and/or the editor(s). MDPI and/or the editor(s) disclaim responsibility for any injury to people or property resulting from any ideas, methods, instructions or products referred to in the content.